Intrinsic properties of the two replicative DNA polymerases of Pyrococcus abyssi in replicating abasic sites: possible role in DNA damage tolerance?

Adeline Palud, Giuseppe Villani, Stéphane L'Haridon, Joël Querellou, Jean-Paul Raffin, Ghislaine Henneke

HAL Id: hal-00617129

https://hal.univ-brest.fr/hal-00617129v1

Submitted on 5 Sep 2011

1 **INTRINSIC PROPERTIES OF THE TWO REPLICATIVE DNA POLYMERASES OF**

2 **PYROCOCCUS ABYSSI IN REPLICATING ABASIC SITES: POSSIBLE ROLE IN DNA**

3 **DAMAGE TOLERANCE ?**

4

5

6 Adeline Palud[1,2], Giuseppe Villani[3], Stéphane L'Haridon[2], Joël Querellou[1,2], Jean-Paul Raffin[1,2]

7 and Ghislaine Henneke[1,2*]

8

9

10 1. Ifremer, UMR 6197, Laboratoire de Microbiologie des Environnements Extrêmes, BP 70,

11 29280 Plouzané, France.

12 2. Université de Bretagne Occidentale, UMR 6197, Laboratoire de Microbiologie des

13 Environnements Extrêmes, 29280 Plouzané, France.

14 3. Institut de Pharmacologie et de Biologie Structurale, CNRS-Université Paul Sabatier Toulouse

15 III, UMR 5089, 205 Route de Narbonne, 31077 Toulouse cedex, France.

16

17 Running Tittle : DNA synthesis by *Pab*pols of DNA containing abasic sites

18

19

20 [*]Corresponding author: Ghislaine HENNEKE, Ifremer, DEEP/LMEE, B.P. 70, 29280 Plouzané,

21 France; Tel.: +33 2 98 22 46 09; Fax: +33 2 98 22 47 57

22 E-mail: ghenneke@ifremer.fr

23

SUMMARY

Spontaneous and induced abasic sites in hyperthermophiles DNA have long been suspected to occur at high frequency. Here, *P.abyssi* was used as an attractive model to analyse the impact of such lesions onto the maintenance of genome integrity. We demonstrated that endogenous AP sites persist at a slightly higher level in *P.abyssi* genome compared to *E.coli*. Then, the two replicative DNA polymerases, *Pab*polB and *Pab*polD, were characterized in presence of DNA containing abasic sites. Both *Pab*pols had abortive DNA synthesis upon encountering AP sites. Under running start conditions, *Pab*polB could incorporate in front of the damage and even replicate to the full-length oligonucleotides containing a specific AP site , but only when present at a molar excess. Conversely, bypassing activity of *Pab*polD was strictly inhibited. The tight regulation of nucleotide incorporation opposite the AP site was assigned to the efficiency of the proofreading function, because exonuclease-deficient enzymes exhibited effective TLS. Steady-state kinetics reinforced that *Pab*pols are high-fidelity DNA polymerases onto undamaged DNA. Moreover, *Pab*pols preferentially inserted dAMP opposite an AP site, albeit inefficiently. While the template sequence of the oligonucleotides did not influence the nucleotide insertion, the DNA topology could impact on the progression of *Pab*pols. Our results are interpreted in terms of DNA damage tolerance.

INTRODUCTION

The genome of a living cell continuously undergoes a plethora of both exogenous or endogenous genotoxic attacks. Among the myriad of DNA lesions, the abasic [apurinic/apyrimidinic (AP)] sites are one of the most common lesions arising at high steady-state levels, yielding up to 2,000-10,000 lesions per human cell per day by spontaneous hydrolysis of the N-glycosylic bond (Lindahl and Nyberg, 1972; Lindahl, 1993). These lesions can be generated by direct elimination of bases via free radical attacks, as a consequence of cells exposure to chemical and physical agents (Breen and Murphy, 1995; Cadet *et al.*, 1999; Loeb *et al.*, 1986). Furthermore, AP sites appear transiently as intermediates of Base Excision Repair (BER) by DNA N-glycosylases (Loeb *et al.*, 1986; Scharer and Jiricny, 2001). Despite the fact that it could be considered as an attractive model, identification and determination of the mutagenic properties of AP sites in hyperthermophilic archaea (HA) remains poorly understood. Presumably, life at high temperature inflicts additional stress to genomic DNA in each cell and very high rates of potentially mutagenic DNA lesions (deamination, depurination, oxidation by hydrolytic mechanisms and subsequent strand breakage) should be expected. However, and interestingly, it was demonstrated that the hyperthermophilic crenarchaeon *Sulfolobus Acidocaldarius* exhibits a modest rate of spontaneous mutations nearly close to that of *Escherichia coli* (*E. coli*), raising the question of how HA do to preserve their genome intact in such deleterious environmental conditions (Grogan *et al.*, 2001; Jacobs and Grogan, 1997).

To cope with the huge spectrum of impediments that result in genome destabilizing lesions, multiple DNA repair mechanisms have evolved in all organisms to ensure genomic stability (Friedberg *et al.*, 2006; Grogan, 2004; Hoeijmakers, 2001). However, situations can arise in which DNA damage escapes to DNA repair and persists into the genome. Cells have developed

65 DNA damage tolerance mechanisms to tolerate hurdles in DNA either by post-replicative gap

66 filling, copy-choice DNA synthesis or translesion DNA synthesis (TLS) (Friedberg, 2005;

67 Friedberg *et al.*, 2006). Both bacteria and eukaryotes can tolerate arrested DNA replication by

68 template switching, therefore avoiding accumulation of mutations (Courcelle *et al.*, 2003;

69 McGlynn and Lloyd, 2002). Whereas template switching systems remain unknown in archaea,

70 TLS appears to be conserved within the three kingdoms of life (Boudsocq *et al.*, 2001; Friedberg

71 *et al.*, 2000; Hubscher *et al.*, 2002; Nohmi, 2006; Pages and Fuchs, 2002; Shimizu *et al.*, 2003;

72 Yang and Woodgate, 2007). Kinetically, this damage tolerance mechanism can be divided in two

73 steps: (i) nucleotide insertion opposite the DNA lesion; (ii) extension beyond the lesion.

74 Depending on the nature of the lesion, the bypass may involve a single or the concerted action of

75 DNA polymerases (Friedberg, 2005; Friedberg *et al.*, 2005). High-fidelity replicative DNA

76 polymerases in crenarchaea, bacteria and eukaryotes are intrinsically severely blocked upon

77 incorporation opposite a lesion such as an abasic site, thus recognizing the illegitimate formed

78 base pair and entering into futile cycles of insertion/excision (Gruz *et al.*, 2003; Pages *et al.*,

79 2005; Tanguy Le Gac *et al.*, 2004; Zhao *et al.*, 2004). This phenomenon called 'idling' is

80 relevant to replicative DNA polymerases harbouring the proofreading 3'-5' exonuclease and

81 reflects the partitioning of a mispaired DNA template between the exonuclease/polymerase

82 active sites (Villani *et al.*, 1978). The exonuclease activity acts as a kinetic barrier to TLS by

83 preventing the stable incorporation of bases opposite the DNA lesion and, therefore, confers the

84 exquisite accuracy of replicative DNA polymerases to preserve the integrity of the genome

85 (Khare and Eckert, 2002). In the absence of coding information due to the base loss, most of

86 replicative DNA polymerases obey to the A-rule, preferentially incorporating a dAMP opposite

87 the abasic site (Haracska *et al.*, 2001; Lawrence *et al.*, 1990; Shibutani *et al.*, 1997).

88 Conceivably, the DNA sequence context, the structure of the DNA primer lesion and the

89 replicative DNA polymerase examined can account for the preferential dAMP insertion opposite

90 an abasic site. Currently, the A-rule for replicative DNA polymerases remains under intensive

91 debates (Hogg *et al.*, 2004; Kroeger *et al.*, 2006; Taylor, 2002).

92 Here, we used *Pyrococcus abyssi* (*P. abyssi*), as a model for studying the genomic maintenance

93 at high temperature. This euryarchaeote grows at an optimum of 95°C and is faced to

94 environmental fluctuations imposed by hydrothermal vents (Erauso *et al.*, 1993; Jolivet *et al.*,

95 2003). Interestingly, *P. abyssi* is able to duplicate bidirectionally its 1.7 million base-pairs from a

96 single origin as fast as 45 minutes (Myllykallio *et al.*, 2000) and DNA replication is thought to

97 be achieved by the two high-fidelity DNA polymerases (*Pab*polD and *Pab*polB) and their

98 accessory factors (Henneke *et al.*, 2005; Rouillon *et al.*, 2007). Consistent with the existing

99 translesional systems and the lack of specialised DNA polymerases in *P. abyssi,* we speculate

100 that one or both *Pab*pols could be involved in damage tolerance. In this study, we determine the

101 steady-state level of AP sites in *E. coli* and *P. abyssi* at different growth stages. Secondly, we

102 examine the bypass properties of the exonuclease proficient and deficient replicative *Pab*pols

103 across an abasic site by varying the DNA topology and sequence context. Finally, steady-state

104 kinetic was employed to give substantial insights into the role of the proofreading activity of

105 *Pab*pols for nucleotide incorporation on damaged in comparison with intact DNA templates.

106 Potential mutagenicity of abasic sites and more generally genomic maintenance in *P. abyssi* are

107 discussed.

108   **RESULTS**

109   **Rate of endogenous AP sites in *P. abyssi* and *E. coli***

110   Before dissecting the *in vitro* behaviour of the *Pab*pols in the presence of abasic sites, we

111   investigated whether such DNA lesions were present into the genome of *P. abyssi.* The

112   mesophilic bacteria *E. coli* was used as a control. The steady-state level of abasic sites was

113   evaluated during the exponential and stationary phases of growth (Figure 1). In the exponential

114   phase, 2 and 25 abasic sites per 100,000 bp were calculated for *E. coli* and *P. abyssi*, respectively

115   (Figure 1). This value moderately increased to reach the number of 4 and 42 abasic sites per

116   100,000 bp at the stationary phase, for *E. coli* and *P. abyssi*, respectively. Taken together, these

117   data provided evidence for the first time that the genome of the hyperthermophile *P. abyssi* has

118   to deal with the presence of abasic sites. Further, the level of AP sites in *P. abyssi* genome is

119   approximately 10-fold higher than in *E. coli*.

120

121   **Replication of AP sites containing M13mp18 DNA template by *Pab*pols**

122   We first checked the capacity of *Pab*pols to duplicate a circular AP-containing

123   heteropolymeric M13mp18 DNA template. Preparation of this damaged AP-M13mp18 templates

124   is depicted in Figure 2A. Under the conditions employed, 11 apurinic (the predominant lesion)

125   and apyrimidinic sites are introduced per molecules (Schaaper and Loeb, 1981). *Pab*pols were

126   tested in a primer extension assay in the presence of either abasic or undamaged M13mp18

127   templates. DNA elongation of the 5'-end fluorescein labelled oligonucleotide 6 (Table 1) was

128   visualized by product analysis on alkaline agarose gel. In the presence of undamaged DNA

129   template, both *Pab*pols (wild-type or exonuclease-deficient, respectively, exo+ and exo-) could

130   extend the primer but with distinct efficiencies. While *Pab*polB exo+/exo- carried out DNA

131   synthesis to the full-length of the unmodified M13mp18 (7,249-nt), *Pab*polD exo+/exo- did only

132   extend the primer to 3,600-nt likely due to its sensitivity to secondary structures as already

133   observed (Henneke *et al.*, 2005) (Figure 2B, compare lanes 2 and 4 to 7 and 9). However, when

134   *Pab*polD exo- elongated the undamaged template, a faint band corresponding to the full-length

135   product was observed (Figure 2B, lane 9), consistent with the lower sensitivity of the *Pab*polD

136   exo- to secondary structures. DNA synthesis reactions of the wild-type *Pab*pols with AP

137   templates gave patterns similar to those obtained with undamaged templates, but with a lower

138   amount of elongated products (Figure 2B, lanes 3 and 8). Therefore, the presence of abasic sites

139   has an inhibitory effect on *Pab*pols activities. The results obtained with *Pab*pols were compared

140   to those of T4 DNA polymerase, used as a control. While the relative distribution of the products

141   of DNA replication was different with damaged versus undamaged M13mp18 DNA template,

142   the lower efficiency of the T4 DNA polymerase (family B) in the presence of DNA lesions was

143   confirmed (Figure 2B, lanes 12 and 13), as already described (Blanca *et al.*, 2007; Tanguy Le

144   Gac *et al.*, 2004). It should be noted that, when reactions were carried out in the presence of

145   *Pab*pols exo- with damaged DNA, a higher amount of replicated DNA products appeared

146   (Figure 2B, compare lanes 3 to 5 for *Pab*polB and lanes 8 to 10 for *Pab*polD) indicating that the

147   proofreading activity of *Pab*pols acts as a kinetic barrier to translesion synthesis onto damaged

148   M13mp18. To further address the inhibitory effect of AP sites onto the DNA polymerising

149   activity of *Pab*pols, quantitative analyses were performed by acid precipitable assay as described

150   under Experimental procedures. Figure 2 C shows the results of replicating these DNA templates

151   by *Pab*pols. Both *Pab*pols could discriminate between damaged and intact M13mp18 DNA

152   template. Indeed, reduced synthetic rates were observed for *Pab*pols independently of the

153   proficient or deficient exonuclease activity, with damaged DNA templates. The presence of AP

154   sites caused a more pronounced inhibition of replication by *Pab*polD, showing a 183-fold and

155   55-fold reduction of synthetic rates, respectively, for *Pab*polD exo+ and *Pab*polD exo-. In the

156   case of *Pab*polB, a 6-fold and 5-fold reduction of synthetic rates, respectively, for *Pab*polB exo+

157   and *Pab*polB exo-, were caused by AP sites. T4 DNA polymerase (family B), used as a control,

158   exhibited a reduced replicating activity comparable to that of *Pab*polB. Taken together, these

159   results argued that *Pab*pols discriminate between undamaged or damaged DNA templates, with

160   distinct reduced polymerising activities, suggesting that the presence of AP sites is rate-limiting.

161

162   **Replication of AP-containing mini-circular and linear oligonucleotides DNA templates by**

163   **the wild-type or exonuclease-deficient *Pab*polB**

164   Since we provided evidence that DNA synthesis was severely impaired on damaged

165   M13mp18 for both *Pab*pols, we further investigated the insights of such reduced activities.

166   Translesional synthesis of a unique AP site from wild-type or exonuclease-deficient *Pab*pols

167   were examined under running start conditions using either linear or mini-circular

168   oligonucleotides DNA templates. The presence of the AP site was controlled by using T4 DNA

169   polymerase as already described (Blanca *et al.*, 2007). While *Pab*polB exo+ could bypass the

170   abasic site with moderate efficiency (63%) at a ratio enzyme / DNA of 4:1, under these

171   conditions *Pab*polB exo- displayed almost full translesion synthesis (93%) (Figure 3A, compare

172   lanes 7 and lanes 14, respectively for *Pab*polB exo+ and *Pab*polB exo-). Moreover, *Pab*polB

173   exo+ had an increased capacity to stall at the AP site, as showed by the more marked presence of

174   pausing sites at the lesion (Figure 3A, lanes 3-7). The efficiency of the bypass was dependent on

175   the amount of the DNA polymerase used and the presence or absence of the 3'- to 5'

176   exonuclease but, in all cases, a plateau could be reached near the equimolar enzyme / DNA

177 concentrations (Figure 3A, lanes 4-5 and lanes 11-12, respectively for *Pab*polB exo+ and

178 *Pab*polB exo-). The tolerance of the abasic site was reproducible and confirmed by using a linear

179 73-mer with a different DNA sequence context (data not shown) as already described (Tanguy

180 Le Gac *et al.*, 2004). When replicating the circular DNA template, the translesion ability of

181 *Pab*polB exo+/exo- was reduced at all enzyme concentrations tested. Interestingly, even at the

182 highest concentrations of *Pab*polB over the minicircle template, translesion synthesis across the

183 AP site for *Pab*polB exo+ only reached 32% at its peak (Figure 3B, lane 7) whereas it was much

184 more effective, reaching up to 86% for *Pab*polB exo- (Figure 3B, lane 13). In addition, under

185 these saturating conditions, there was a stimulation of strand displacement activity of the two

186 *Pab*polB versions, as indicated by the proportion of products longer than the 87-mer (Figure 3B,

187 lane 6-7 and 12-13). Taken together these results indicate that *Pab*polB has the capacity to

188 replicate past an AP site at high pol/DNA ratio. The proofreading activity of *Pab*polB influences

189 its translesion capacity and progression of both exonuclease-deficient and proficient *Pab*polB are

190 reduced in the presence of the mini-circular DNA template.

191

192 **Replication of AP-containing mini-circular and linear oligonucleotides DNA template by**

193 **the wild-type or exonuclease-deficient *Pab*polD**

194   The ability of *Pab*polD exo+/exo- to bypass an abasic site onto the linear and circular

195 oligonucleotides DNA templates was analysed and the results are presented in Figure 4. As it can

196 be seen, *Pab*polD exo+ could incorporate in front of the AP site but, contrary to *Pab*polB, could

197 not extend past the lesion both on linear and circular DNA templates at all the enzyme's

198 concentrations tested (lanes 3-7 in Figure 4A, and in Figure 4B). In addition, accumulation of a

199 shorter product at position +32 could be detected, indicating the 'idling' activity of the *Pab*polD

200   exo+. *Pab*polD exo- was also blocked at the AP site in the presence of the linear template but

201   longer products past the AP site at position + 34, + 35, and + 36 could be detected, although they

202   never reached the full-length of the 87-mer, even at saturating enzyme concentrations (Figure

203   4A, lanes 9-13). Interestingly, 35% of bypass could be measured at a ratio *Pab*polD exo - / DNA

204   of 4:1 on the linear DNA template. Similarly, when the experiments were repeated in the

205   presence of the minicircle DNA template, a strong block at the AP site (+ 33) could be observed

206   for *Pab*polD exo - present at lower concentration to the DNA template (Figure 4B, lanes 9-10).

207   Moreover, DNA synthesis continued past the AP site at position + 34, + 35, and + 36, but was

208   also able to reach up to the full-length 87-mer (Figure 4B, lanes 11-13), when the concentration

209   of the enzyme was higher than that of the minicircle DNA template. Therefore, in the case of

210   *Pab*polD, its exonuclease activity prevents translesion synthesis of an abasic site independently

211   of the structure of DNA template, while the exo − mutant shows some bypass capacity that

212   seems enhanced in the case of a mini-circular DNA.

213

214   **Steady-state kinetic analysis of nucleotide incorporation of wild-type and exonuclease-**

215   **deficient *Pab*pols opposite undamaged bases**

216   *Pab*pols have been designated as replicative DNA polymerases (Henneke *et al.*, 2005).

217   This designation supposes that *Pab*pols must endow with high selectivity for each incoming

218   nucleotide depending on the nature of the base-containing template. Nucleotide incorporation

219   kinetics were measured in standing start reactions as described in Experimental procedures.

220   Incorporation efficiency (k_{cat}/K_m) were measured for the wild-type and exonuclease-deficient

221   *Pab*pols and the frequency of nucleotide misinsertion was calculated as the ratio of the efficiency

222   (k_{cat}/K_m) of incorrect nucleotide incorporation to the efficiency (k_{cat}/K_m) of correct nucleotide

223   incorporation (Table 2). Both wild-type *Pab*pols exclusively incorporated the correct dGMP

224   opposite template C and no misincorporation could be detected. In these conditions, a 5-fold

225   reduced incorporation efficiency for *Pab*polD compared to *Pab*polB was observed as indicated

226   by the k_{cat}/K_m values. The results obtained with the exonuclease-deficient *Pab*pols at template C

227   showed that the correct dGMP was preferentially incorporated but their efficiencies were

228   dramatically reduced compared to the wild-type enzymes, as judged from the dropped k_{cat}/K_m

229   values, 55- and 103-fold, respectively, for *Pab*polB and *Pab*polD. In addition, misinsertion

230   events by the exonuclease-deficient *Pab*pols at template C were comparable, with preference for

231   insertion of dTMP > dAMP > dCMP (Table 2). Taken together, these results demonstrate that,

232   while wild-type *Pab*pols monitor the instructional base of the template and discriminate between

233   correct and incorrect nucleotides insertion, exonuclease-deficient *Pab*pols are much less

234   efficient.

235

236   **Steady-state kinetics analysis of nucleotide incorporation of wild-type and exonuclease-**

237   **deficient *Pab*pols opposite an AP site**

238   The efficiency for deoxynucleotide insertion opposite an abasic site for the wild-type

239   *Pab*polB followed the order dAMP > dTMP and to a lesser extent dGMP. Interestingly, *Pab*polB

240   exo + incorporated a dGMP 8355-fold less efficiently opposite an AP site than opposite the

241   template C (Table 2). Similarly, as judged by the k_{cat}/K_m values, *Pab*polD exo + incorporated

242   preferentially a dAMP over a dTMP opposite the abasic site with a 20-fold higher magnitude

243   efficiency. It is noteworthy that the apparent K_m values from the incorporation of nucleotides

244   opposite the abasic site were always higher than from the insertion of a correct dGMP at

245   template C. Thus, proficient proofreading *Pab*pols are sensitive to abasic sites and are not

246   efficient at inserting a nucleotide opposite such a non-instructive lesion. As observed from the

247   k_{cat}/K_m values, *Pab*pols exo - inserted a dAMP more efficiently than other deoxynucleotides

248   opposite the AP site. While incorporation efficiencies of dAMP, dGMP and dTMP were higher

249   when the proofreading function of *Pab*polB was deficient, no striking difference was observed

250   between the wild-type and exonuclease-deficient *Pab*polD. Therefore, *Pab*polB and *Pab*polD

251   exonuclease-deficient resemble each other in their ability to insert nucleotides opposite an abasic

252   site with higher efficiencies for dAMP incorporation. Taken together, the data show that, while

253   wild-type *Pab*polB does not significantly discriminate among nucleotides for incorporation

254   opposite an AP site, the exonuclease-deficient *Pab*polB and both wild-type and exonuclease-

255   deficient *Pab*polD were much sensitive to a non-coding lesion that seems to govern the dAMP

256   incorporation rather than other dNTPs.

257

258   **Effect of varying the downstream template base on nucleotide incorporation opposite an**

259   **AP site by the *Pab*pols**

260   The primer-templates used in these experiments were designed in order to examine the

261   effect of changing the template base (N) at the 5' side of the AP site (X) on the initiation of the

262   extension of the primer. Nucleotide incorporation was measured in standing start reactions under

263   standard *Pab*pols assay conditions. The 32-mer primer (oligonucleotide 6) was annealed to the

264   four templates differing by the nature of the base N = A, T, G and C at the 5' side of the AP site

265   (Oligonucleotides 2, 1, 3, 4, respectively) (Figure 5). Extension of the primer in the four

266   duplexes was conducted in the presence of each of the natural dNTPs. On the one hand, the wild-

267   type *Pab*pols exclusively inserted a dAMP opposite the abasic lesion, independently of the

268   sequence context (Figures 5A and 5B). While the percentages of incorporation of a dAMP

269   ranged from 46 to 58% for *Pab*polD exo+, they only reached 18% for *Pab*polB exo+. The

270   *Pab*pols exo- also preferentially incorporated a dAMP opposite the AP site with a higher order of

271   magnitude compared to the *Pab*pols exo+. For example, the percentages of incorporation of a

272   dAMP ranged from 66 to 72% for *Pab*polD exo- and 46 to 58% for *Pab*polD exo+ (Figure 5D

273   and Figure 5B, respectively). However, unlike *Pab*pols exo+, the *Pab*pols exo- also inserted

274   other   dNMPs   opposite   the   non   instructional   lesion,   following   the   order:

275   dAMP>dGMP>dTMP>dCMP for *Pab*polB exo- and dAMP>dTMP~dCMP>dGMP for *Pab*polD

276   exo-, independently of the sequence context (Figures 5C and 5D, respectively). Thus, these

277   results demonstrate that nucleotide incorporation opposite an AP site by the *Pab*pols exo+/exo-

278   is not directed by the nature of the base located at the 5' side of the AP site.

279 **DISCUSSION**

280   In hyperthermophiles, cellular and environmental stresses encountered by cells are likely

281 to be exacerbated by adaptation to extreme conditions. Cell survival is ensured by a complex

282 network of DNA events that contributes to the maintenance of the functional integrity of nucleic

283 acids at high temperature. Here, we have focused the study on *P. abyssi*, an anaerobe

284 hyperthermophilic euryarchaeota (HA) that thrives at elevated temperature in the immediate

285 surroundings of deep-sea hydrothermal vents. This is the first report that establishes a

286 relationship between the specific genomic level of abasic sites and the resulting impact on the

287 intrinsic properties of replicative DNA polymerases in archaea. These features show that *P.*

288 *abyssi* can be used as an informative model to analyse the biological relevance of DNA damage

289 accumulation in the hyperthermophilic chromosome and the underlying genomic maintenance

290 mechanisms.

291   The investigation presented here shows that the steady-state level of AP sites into the 1.7

292 million base-pairs of *P. abyssi* ranged from 25 to 42 AP sites per 100,000 bp during the

293 exponential and stationary phases, respectively. Similarly, a 2-fold increase of AP sites is

294 observed in *E. coli*. These findings corroborate the higher efficiency of DNA protection and

295 repair mechanisms in proliferating cells, compatible with a low level of AP sites. However, it is

296 important to precise that our expectation to detect a drastic increased number of abasic sites in

297 the hyperthermophilic chromosome was not fulfilled. Indeed, the level was only 10-fold higher

298 than in the mesophilic bacteria *E. coli*. Comparatively, the frequency of endogenous AP sites in

299 mammalian cells reached 10 to 12 AP sites per 100,000 bp (Zhao *et al.*, 2006). Indeed, in the

300 literature, the number of AP sites in the genome of thermophilic and hyperthermophilic

301 microorganisms is always suspected to increase drastically compared to the mesophilic

302 counterparts (Grogan, 1998; Grogan, 2000). This assumption takes into account of the intrinsic

303 properties of the primary structure of DNA at elevated temperatures, corresponding to a 3,000-

304 fold increase in DNA decay at 100°C (Lindahl, 1993). Conceivably, *P. abyssi* has evolved to

305 adjust genetically the level of endogenous AP sites in its genome that could be detrimental for

306 genome integrity of mesophiles. Accumulation of AP sites and, more generally, others DNA

307 lesions can be envisaged, suggesting that hyperthermophiles are adapted to survive pre-existing

308 mutations. Clearly, these results establish that the number of AP sites seems to evolve respect to

309 the growth stage without affecting cell growth and viability. However, further studies are

310 required to determine the threshold that hyperthermophiles can support to ensure cell survival.

311 Evolution has produced multiple DNA polymerases able to replicate undamaged or

312 damaged DNA. Sixteen DNA polymerases have been described in human, nine in

313 *Saccharomyces cerevisiae*, five in *E. coli* (Bebenek and Kunkel, 2004; Hubscher *et al.*, 2002;

314 Rothwell and Waksman, 2005) and up to five in archaea (Barry and Bell, 2006; Yang, 2005).

315 Interestingly, the genome of the euryarchaeota *P. abyssi* encodes only two DNA polymerases,

316 families B and D, required to faithfully duplicate the genetic information (Henneke *et al.*, 2005).

317 In this study, steady-state kinetic analyses of nucleotide insertion show for the first time that

318 *Pab*polD is endowed with high-fidelity onto undamaged DNA as its replicative counterpart,

319 *Pab*polB (Table 2). Incorporation efficiency of *Pab*polD was reduced to five fold compared to

320 *Pab*polB, demonstrating that *Pab*pols possesses distinct kinetic properties.

321 Our results give evidence that the presence of AP sites strongly inhibited the DNA polymerising

322 activity of both *Pab*pols and that the absence of their proofreading function correlate with

323 enhanced bypass of AP sites. The degree of inhibition of DNA synthesis was dependent upon the

324 *Pab*pol examined. *Pab*polD could insert a nucleotide opposite the AP site and, in all conditions

325   tested, was not able to extend beyond the 3' primer lesion. *Pab*polB inserted opposite the AP site

326   and extended the DNA template to the full-length, only when present at a molar excess over the

327   template. This result is comparable to previous studies showing that molar excess of enzyme

328   versus DNA template could enhance translesion synthesis by DNA polymerases past an abasic

329   site (Blanca *et al.*, 2007; McCulloch and Kunkel, 2006; Tanguy Le Gac *et al.*, 2004). While

330   translesion synthesis of both exonuclease-proficient and deficient *Pab*polBs and the exonuclease-

331   deficient *Pab*polD were differently affected by the topology of the DNA template, the template

332   sequence context did not significantly influence the bypass properties of *Pab*pols. Further, both

333   *Pab*pols inserted dAMP opposite the AP site independently of the nature of the 5' template base

334   to the AP site. Despite this nucleotide selectivity, steady-state kinetics showed that dAMP

335   incorporation was not efficient. These observations show for the first time that archaeal

336   replicative (families B and D) DNA polymerases follow the 'A-rule' (Strauss, 1991; Taylor,

337   2002) like eukaryal and bacterial counterparts (Haracska *et al.*, 2001; Shibutani *et al.*, 1997). The

338   physical basis of the 'A-rule' is still an intensive debate (Kool, 2002; Zahn *et al.*, 2007) and

339   structural studies reported the molecular level of replication blockage that produced catalytically

340   inactive DNA polymerases (Freisinger *et al.*, 2004; Hogg *et al.*, 2004). Whether the molecular

341   and physical bases are conserved through archaeal replicative DNA polymerases would have to

342   be unravelled. Accordingly, the ability of abasic sites to inhibit *Pab*pols could reflect steric

343   constraints imposed by the "tightness" of the active site. Furthermore, the capacity to partition

344   the mispairs away from the polymerase domain into the exonuclease active site might exhibit

345   structural rearrangements that are differentially influenced by the dynamic features of the DNA

346   polymerase. To this point, the major distinction between the two *Pab*pols is the subunits

347   composition. While *Pab*polB is a monomeric enzyme with associated exonuclease and

348 polymerase activities, *Pab*polD is an heterodimeric enzyme with the large and the small subunits

349 carrying, respectively, the polymerase and the exonuclease activities (Gueguen *et al.*, 2001).

350 Therefore, it is reasonable to suggest that the architecture of the two DNA polymerases may

351 account for the subtle differences observed within the polymerase and exonuclease efficiencies.

352 However, a complete detailed functional analysis must await the crystal structure of the

353 individual *Pab*pols. The balance between polymerization and excision was recently described in

354 B-family DNA polymerase in archaea (Kuroita *et al.*, 2005) but never in D-family. The distinct

355 kinetic partitioning of insertion and edition of mispairs observed within *Pab*pols corroborates

356 with eukaryal and bacterial homologues properties (Jin *et al.*, 2003; Jin *et al.*, 2005; Pages *et al.*,

357 2005) and confers that replicative DNA polymerases are high-fidelity enzymes (Bloom *et al.*,

358 1997; Chen *et al.*, 2000; Shimizu *et al.*, 2002).

359 The down-regulation of the proofreading function of *Pab*polB could favour TLS in order to

360 overcome the block imposed by AP sites. Bypass of AP sites could generate either single-base

361 substitutions or frameshift mutations (Baynton and Fuchs, 2000). *Pab*polB appears to proceed

362 through single-base substitution upon completion of DNA template containing an AP site. The

363 molar excess of the enzyme over the DNA template accounted for TLS under our *in vitro*

364 conditions. On the other hand, a replicative *Pab*pol idling at a DNA lesion could be a crucial

365 factor to trigger cellular responses to DNA damage in *P. abyssi*. The mechanism by which

366 proofreading activities of archaeal DNA polymerases could be regulated *in vivo* (dNTPs balance,

367 role of accessory proteins and enzymes switching) and their contribution in some cases to

368 counteract genomic DNA lesions has to be elucidated. Recently, it was described that *P. abyssi*

369 has evolved with efficient DNA strategies to cope with ionizing radiations and elevated

370 temperatures (Jolivet *et al.*, 2003). Biochemical evidence for relevant DNA repair mechanisms

371   has not been demonstrated in *P. abyssi* yet. More striking is the lack of identification of any

372   mismatch repair genes and the complete set of damage excision genes (Cohen *et al.*, 2003).

373   Interestingly, homologous recombination genes (RecA/Rad51) have been identified into the

374   genome sequence of *P. abyssi* together with the fact that exponentially growing thermophilic

375   archaea contain several copies of the chromosome (Bernander and Poplawski, 1997; Breuert *et

376   al.*, 2006). This might be particularly consistent for the repair of strand breaks. Furthermore, it is

377   not excluded that the recently characterised primase from *P. abyssi* could also play a role in

378   damage avoidance since it possesses sequence and structural similarities with the family X DNA

379   polymerases (Le Breton *et al.*, 2007). Ultimately, the process of such DNA lesions would have to

380   be explored by the *P. abyssi* replisome in the context of genomic mutagenicity.

381 **EXPERIMENTAL PROCEDURES**

382 **Strains and cell culture techniques**

383 *P. abyssi* GE5 (Brittany Culture Collection, http://www.ifremer.fr/souchotheque) were

384 grown in 50 ml YPS medium under anaerobic conditions at 95°C (Erauso *et al.*, 1993). The *E.*

385 *coli* CIP 54.8 strain (CRBIP) was cultivated in 1 L of Luria-Bertani (LB) broth (1% tryptone,

386 0.5% yeast extract, 1% NaCl) at 37°C and pH 7.3, in a shaking incubator (170 rpm). Growth was

387 monitored by density measurements with a cell Thoma counting chamber (0.02 mm depth).

388 Samples for DNA extraction were collected in the exponential and stationary growth phases as

389 indicated in Figure 1. The samples for DNA extraction were centrifuged at 6,000 g for 15 min at

390 4°C and the pellets were stored at −20°C.

391

392 **Genomic DNA Isolation and Detection of AP sites**

393 Genomic DNA from *P. abyssi* was isolated using the extraction method as described

394 (Charbonnier *et al.*, 1995) and optimised in order to avoid the formation of additional AP sites.

395 Briefly, cell pellets were suspended in 800 µl TE-Na-1 X lysis buffer (100 mM Tris-HCl, 50 mM

396 EDTA, 100 mM NaCl, pH 8.0). This was followed by successive additions of 50 µl proteinase K

397 (20 mg/ml), 100 µl Sarcosyl (10%), 100 µl SDS (10%). The applied lysis treatment were

398 performed at 37°C for 1.5 hours and isolation of the total DNA was accomplished by adding an

399 equal volume of buffered (pH 8.0) PCI (Phenol/Chloroform/Isoamyl Alcohol: 25/24/1). The

400 samples were gently mixed and the aqueous phases were collected by centrifugation at 10,000 g

401 for 10 min at 4°C. 10 µl RNAse (10 mg/ml) were added and incubation was performed at 37°C

402 for one hour. DNAs were purified with an equal volume of PCI and centrifuged. The upper phase

403 was extracted with an equal volume of pure chloroform and centrifuged. DNA precipitation was

404   obtained by mixing the final aqueous phase with 0.7 volume of 100% isopropanol followed by

405   incubation for one hour at room temperature. After a 30 min centrifugation at 15,000 g at 4°C,

406   the DNA pellets were washed once with 0.5 ml of 70% ice cold ethanol. Finally, the DNA pellets

407   were air-dried during 1 hour before solubilization in TE-1X buffer (10 mM Tris-HCl, 2 mM

408   EDTA, pH 7.5).

409   Genomic DNA extractions from *E. coli* was performed following the CTAB (Hexadecyl

410   trimethyl-ammonium bromide) method for Gram-negative bacteria as described (Park, 2007).

411   The level of AP sites in genomic DNA was measured using the DNA damage

412   quantification –AP site Counting kit from Dojindo Molecular Technologies (Gaithersburg, MD).

413   DNA pellets were dissolved in TE buffer supplied by the kit and DNA concentrations were

414   exactly adjusted to 100 ng/μl. Briefly, DNA samples were incubated with the Aldehyde Reactive

415   Probe (ARP) reagent (N'-aminooxymethylcarbonylhydrazino-D-biotin) that specifically reacted

416   with the aldehydic ring-opened AP sites (Kow and Dare, 2000; Kubo *et al.*, 1992). The AP sites

417   tagged with biotin interacted with horseradish peroxidase-streptavidin and AP sites were

418   colorimetrically detected. For each condition, the average of three measurements per sample was

419   used in the statistical analyses.

420

421   **Chemicals and Enzymes**

422   Unlabelled dNTPs were from MP Biomedicals. T4 polynucleotide kinase, DNA ligase

423   and T4 DNA polymerase were from New England Biolabs. *Pab*polD was cloned, expressed and

424   purified as described (Henneke *et al.*, 2005). *Pab*polB (Isis DNA polymerase) and *Pab*polB

425   exonuclease-deficient (Pyra DNA polymerase) were purchased from MP Biomedicals. 1 unit of

426   *Pab*pols corresponds to the incorporation of 1 nmol of total dTMP into acid–precipitable

427   material per min at 65°C in a standard assay containing 0.5 µg (nucleotides) of

428   poly(dA)/oligo(dT)$_{10:1}$. All other reagents were of analytical grade and purchased from Sigma-

429   Aldrich and Fluka.

430

431   **Construction, expression and purification of the recombinant wild-type and exonuclease-**

432   **deficient His tag *Pab*polD**

433   The pET26b expression vector containing the *Pab*polD large subunit (DP2) (Gueguen *et*

434   *al.*, 2001) was digested with *Nde*I and *Sal*I and the resulting fragment was inserted into the

435   pET28a expression vector (Novagen) in order to introduce a histidine tag (His tag) at the N-

436   terminus. To render the *Pab*polD exonuclease-deficient, site-directed mutagenesis was carried

437   out by introducing the H451A point mutation onto the *Pab*polD small subunit (DP1) (Gueguen *et*

438   *al.*, 2001). The two site-specific complementary primers, reverse H451A 5'-

439   TGGCCTAGCGGCATCGGCATTTCCTGGCCCTAT-3' and forward H451A 5'-

440   ATAGGGCCAGGAAATGCCGATGCCGCTAGGCCA-3' were used to PCR amplify the

441   pARHS expression vector containing DP1 according to the protocol of the Quick change

442   Mutagenesis kit (Stratagene, La Jolla, CA). DNA sequencing was used to confirm that no

443   spurious mutations had been introduced during PCR. The constructed expression vectors

444   pET28a/DP2 and either the wild-type or the exonuclease-deficient pARHS/DP1 were co-

445   introduced into host *E. coli* HMS174 (DE3). The transformed cells were grown in 1.5 liters Luria

446   Bertani (LB) medium containing ampicillin (100 µg/ml) and kanamycin (30 µg/ml) at 37 °C.

447   When A_{600} reached 0.7, 1 mM isopropylthio-β-D-galactoside was added to induce expression of

448   active DNA polymerases. After being cultured 4 hours at 37 °C with gentle shaking (160 rpm),

449   the cells were harvested by centrifugation, resuspended in 25 ml buffer A (20 mM sodium

450   phosphate, pH 6.6, 1 mM DTT, 20 mM Imidazole) containing the protease inhibitor, disrupted

451   on ice by French press and then heat-treated at 80°C for 15 min. Denatured host proteins were

452   removed by centrifugation. The clarified supernatant was applied further onto Ni^{2+}–HisTrap

453   column (5 ml of bed volume) pre-equilibrated with buffer A. Proteins were eluted with buffer B

454   (20 mM sodium phosphate, pH 6.6, 1 mM DTT, 500 mM Imidazole and active fractions were

455   pooled and dialysed against buffer C (20 mM sodium phosphate, pH 6.6, 1 mM DTT). The

456   dialysate was loaded onto a heparin column (5 ml of bed volume) pre-equilibrated with buffer D

457   (20 mM sodium phosphate, pH 6.6, 1 mM DTT, 0.15 M NaCl). The column was developed with

458   a linear gradient from buffer D to buffer E (20 mM sodium phosphate, pH 6.6, 1 mM DTT, 1 M

459   NaCl). Eluted protein showed over 98% purity. Pure His-*Pab*polD (wild-type and exonuclease-

460   deficient) were dialyzed against storage buffer (25 mM Tris–HCl, pH 8.0, 1 mM DTT, and 50%

461   glycerol) and stored at −20 °C until use. We checked by acid precipitable assay, as described

462   (Henneke *et al.*, 2005), that the addition of the His tag at the N terminus of DP2 had no effect on

463   the DNA polymerization activities. Moreover, the 3'-5' exonuclease deficiency for the mutant

464   H451A was confirmed (data not shown). Sequence alignment of exonuclease domain in

465   representative euryarchaeal DNA polymerases highlighting residues critical for proofreading

466   function is shown in Figure S1.

467

468   **Nucleic Acid Substrates**

469   Single-stranded (ss) M13mp18 was purchased (Amersham Biosciences, GE Healthcare).

470   In order to create AP sites into natural DNA templates, the ssM13mp18 viral DNA was

471   incubated at a final concentration of 0.18 pmol/μl in 30 mM potassium chloride, 10 mM sodium

472   citrate, pH 3.0 at 70°C for 45 min (Schaaper *et al.*, 1983). These conditions introduced one AP

473   sites per molecule in 4 min, measured by survival (Schaaper and Loeb, 1981). After treatment,

474   the damaged M13mp18 was purified with the QIAquick® PCR Purification Kit from Qiagen

475   (Germany).

476   The sequences of the DNA primers / templates used in the present study are depicted in

477   Table 1. All oligonucleotides, including those containing a tetrahydrofuran moiety mimicking an

478   abasic site, were chemically synthesized and gel-purified (Eurogentec, Belgium). Primers were

479   labelled at their 5'-end by fluorescein with the 5' End Tag kit labelling system from Vector

480   Laboratories (California). Free fluorescein was removed through the Microspin G-25 column

481   (Amersham Biosciences, GE Healtcare) and the labelled primers were hybridised to the

482   respective templates at equimolar concentrations.

483   The minicircle template was prepared as described (Tanguy Le Gac *et al.*, 2004). Briefly,

484   the linear 5'-phosphorylated oligonucleotide 1 (intact or containing the tetrahydrofuran moiety)

485   was intramolecularly ligated under dilute conditions using a scaffold 40-mer oligonucleotide (5'-

486   ATATTCCTACCCTCCCGATCTATCCACCATACTACCCTCC- 3'). Minicircles were gel-

487   purified and their concentration was determined spectrophotometrically, followed by annealing

488   with their complementary 5'-fluorescein labelled primer at equimolar concentration.

489

490   **Primer extension onto intact or damaged primed-oligonucleotides**

491   "Standing start" and "Running start" assays were catalysed into a final volume (15 μl)

492   containing the following components: (i) for *Pab*polD: 8.3 nM of labelled primers / templates, 20

493   nM of *Pab*polD exo+/exo- unless otherwise specified, 10 mM Tris-HCl (pH 9.0), 50 mM KCl,

494   10 mM $MgCl_2$ and 200 μM dNTPs; (ii) for *Pab*polB: 8.3 nM of labelled primers / templates, 13

495   nM of *Pab*polB exo+/exo- unless otherwise mentioned, 50 mM Tris-HCl (pH 8.8), 50 mM KCl,

496 1 mM DTT, 2 mM MgCl$_2$ and 200 µM dNTPs. Reactions were performed at 55°C for 30

497 minutes and quenched by the addition of 15 µl of stop buffer (98% formamide, 10 mM EDTA).

498 Samples were heated at 95°C for 5 minutes. The reactions products were resolved on 15%

499 polyacrylamide, 7 M urea gels and visualized with a Mode Imager Typhoon 9400 (Amersham

500 Biosciences, GE Healthcare). Quantification of the results was performed using ImageQuant 5.2

501 software. The extent of the bypass reaction was calculated as the ratio of the intensity of the

502 bands downstream of the AP site to the intensity of the bands opposite the lesion.

503   Effect of sequence context on AP site bypass was analysed under standing start

504 conditions. The fluorescein-labelled primer (oligonucleotide 6) was annealed right before the

505 template AP site that is indicated by X. Different template bases 5′ to the AP site are depicted by

506 N (N=A, oligonucleotide 2; N=T, oligonucleotide 1; N=G, oligonucleotide 3; N=C,

507 oligonucleotide 4) (Table 1). Bypass assays were performed as described above excepted that 16

508 nM of DNA templates were used when the template base 5' to the AP site was: N=T and N=C

509 for *Pab*polB exo-, N=T and N=G for *Pab*polD exo+, N=C for *Pab*polB exo+. Quantification of

510 nucleotides insertion opposite the AP site are calculated for wild-type and exonuclease-deficient

511 *Pab*pols in triplicate but only the more resolving gel was quantified.

512

513 **Steady-state Kinetic Analyses**

514   A 5'-fluorescein labelled primer, annealed to either a correct or damaged template, was

515 extended in the presence of increasing concentrations of a single dNTP. *Pab*pols concentrations

516 and reaction times were set so that maximal product formation was ≤ 20% of the substrate

517 concentration. The linear primer-template (oligonucleotides 6 and 1) was extended with dNTP at

518 55°C in the presence of 6.6-33.3 nM enzyme for 1 or 5 min, depending on the proper utilization

519   efficiency and substrate utilisation. All reactions (15 µl) were carried out at various dNTP

520   concentrations (in triplicate) and quenched with 2 volumes of a solution of 20 mM EDTA in 95%

521   formamide (v/v). Products were resolved using a 15% polyacrylamide (w/v) electrophoresis gel

522   containing 7 M urea and visualized using a Mode Imager Typhoon 9400. Bands were quantified

523   with ImageQuant 5.2 software (Amersham Biosciences, GE Healthcare). The observed rates of

524   deoxynucleotide incorporation as a function of dNTP concentration were firstly determined from

525   Lineweaver-Burk plots. The data were fit by nonlinear regression using the Marquardt-

526   Levenberg algorithm (EnzFitter 2.0, BioSoft) to the Michaelis-Menten equation describing a

527   hyperbola, $v = (V\text{max} \times [\text{dNTP}]/K\text{m} + [\text{dNTP}])$ as already described (Le Breton *et al.*, 2007).

528   Apparent Km and Vmax kinetic parameters were obtained from the fit and were used to calculate

529   the efficiency of deoxynucleotide incorporation (k_{cat}/K_m). The kinetics values are the average of

530   at least triplicate determinations and are shown with standard deviations (SD). ND, means that

531   no detectable incorporation was observed. Gel patterns and quantitation of single nucleotide

532   incorporation reactions are shown in Figure S2.

533

534   **Primer extension onto intact or damaged M13mp18 DNA template**

535   *Product analysis*. The oligonucleotide 6 was annealed to either the damaged AP-

536   M13mp18 or undamaged M13mp18 at a molar ratio 3:1. Standard *Pab*pols reactions (10 µl) were

537   conducted into their respective buffer containing 200 µM each of dNTPs, 7 nM of DNA template

538   and 2 pmol of *Pab*pols. Reactions were carried out at 60°C for 30 minutes. T4 DNA polymerase

539   reactions were performed at 37°C for 30 minutes into the 1 X T4 pol buffer (according to the

540   manufacturer's protocol) with 7 nM of DNA template, 100 µM each of dNTPs and 2 pmol of T4

541   DNA polymerase. Reaction mixtures were stopped by the addition of 10 µl of 30 mM EDTA and

542   the samples were heated to 100°C for 10 min. Reactions mixtures were subjected to a 0.8% (w/v)

543   denaturing alkaline agarose gel electrophoresis, and replication products were visualized with a

544   Mode Imager Typhoon 9400 (Amersham Biosciences, GE Healthcare). DNA ladders (Raoul

545   markers, MP Biomedicals) were run into the same gel and revealed separately.

546   *Acid precipitable assay.* The reaction buffers composition were identical to those

547   described in product analysis for *Pab*pols and T4 DNA pol. The final volume of 10 µl contained

548   200 µM of unlabeled dNTPs, 20 µM [^{3}H]dTTP, 7 nM of DNA template (AP-M13mp18 or

549   undamaged M13mp18) and 2 pmol of enzyme to be tested. Reactions were carried out at 60°C

550   and 37°C, respectively, for *Pab*pols and T4 DNA pol for 30 minutes. DNA was precipitated with

551   10% trichloroacetic acid (TCA). Insoluble radioactive material was determined by scintillation

552   counting as described (Henneke *et al.*, 2005; Rouillon *et al.*, 2007).

REFERENCES

Barry, E.R., and Bell, S.D. (2006) DNA replication in the archaea. *Microbiol Mol Biol Rev* **70**: 876-887.

Baynton, K., and Fuchs, R.P. (2000) Lesions in DNA: hurdles for polymerases. *Trends Biochem Sci* **25**: 74-79.

Bebenek, K., and Kunkel, T.A. (2004) Functions of DNA polymerases. *Adv Protein Chem* **69**: 137-165.

Bernander, R., and Poplawski, A. (1997) Cell cycle characteristics of thermophilic archaea. *J Bacteriol* **179**: 4963-4969.

Blanca, G., Delagoutte, E., Tanguy le Gac, N., Johnson, N.P., Baldacci, G., and Villani, G. (2007) Accessory proteins assist exonuclease-deficient bacteriophage T4 DNA polymerase in replicating past an abasic site. *Biochem J* **402**: 321-329.

Bloom, L.B., Chen, X., Fygenson, D.K., Turner, J., O'Donnell, M., and Goodman, M.F. (1997) Fidelity of Escherichia coli DNA polymerase III holoenzyme. The effects of beta, gamma complex processivity proteins and epsilon proofreading exonuclease on nucleotide misincorporation efficiencies. *J Biol Chem* **272**: 27919-27930.

Boudsocq, F., Iwai, S., Hanaoka, F., and Woodgate, R. (2001) Sulfolobus solfataricus P2 DNA polymerase IV (Dpo4): an archaeal DinB-like DNA polymerase with lesion-bypass properties akin to eukaryotic poleta. *Nucleic Acids Res* **29**: 4607-4616.

Breen, A.P., and Murphy, J.A. (1995) Reactions of oxyl radicals with DNA. *Free Radic Biol Med* **18**: 1033-1077.

Breuert, S., Allers, T., Spohn, G., and Soppa, J. (2006) Regulated polyploidy in halophilic archaea. *PLoS ONE* **1**: e92.

581 Cadet, J., Delatour, T., Douki, T., Gasparutto, D., Pouget, J.P., Ravanat, J.L., and Sauvaigo, S.

582   (1999) Hydroxyl radicals and DNA base damage. *Mutat Res* **424**: 9-21.

583 Charbonnier, F., Forterre, P., Erauso, G., and Prieur, D. (1995) Purification of Plasmids from

584   Thermophilic and Hyperthermophilic Archaea. In *Archaea: A Laboratory Manual*. F.T.

585   Robb, A.R.P. (ed): Cold Spring Harbor Laboratory Press, pp. 87-90.

586 Chen, X., Zuo, S., Kelman, Z., O'Donnell, M., Hurwitz, J., and Goodman, M.F. (2000) Fidelity

587   of eucaryotic DNA polymerase delta holoenzyme from Schizosaccharomyces pombe. *J*

588   *Biol Chem* **275**: 17677-17682.

589 Cohen, G.N., Barbe, V., Flament, D., Galperin, M., Heilig, R., Lecompte, O., Poch, O., Prieur,

590   D., Querellou, J., Ripp, R., Thierry, J.C., Van der Oost, J., Weissenbach, J., Zivanovic,

591   Y., and Forterre, P. (2003) An integrated analysis of the genome of the hyperthermophilic

592   archaeon Pyrococcus abyssi. *Mol Microbiol* **47**: 1495-1512.

593 Courcelle, J., Donaldson, J.R., Chow, K.H., and Courcelle, C.T. (2003) DNA damage-induced

594   replication fork regression and processing in Escherichia coli. *Science* **299**: 1064-1067.

595 Erauso, G., Reysenbach, A.L., Godfroy, A., Meunier, J.R., Crump, B., Partensky, F., Baross,

596   J.A., Marteinsson, V., Barbier, G., Pace, N.R., and Prieur, D. (1993) *Pyrococcus abyssi*

597   sp. nov., a new hyperthermophilic archaeon isolated from a deep-sea hydrothermal vent.

598   *Archives of Microbiology* **160**: 338-349.

599 Freisinger, E., Grollman, A.P., Miller, H., and Kisker, C. (2004) Lesion (in)tolerance reveals

600   insights into DNA replication fidelity. *Embo J* **23**: 1494-1505.

601 Friedberg, E.C., Feaver, W.J., and Gerlach, V.L. (2000) The many faces of DNA polymerases:

602   strategies for mutagenesis and for mutational avoidance. *Proc Natl Acad Sci U S A* **97**:

603   5681-5683.

604   Friedberg, E.C. (2005) Suffering in silence: the tolerance of DNA damage. *Nat Rev Mol Cell*

605   *Biol* **6**: 943-953.

606   Friedberg, E.C., Lehmann, A.R., and Fuchs, R.P. (2005) Trading places: how do DNA

607   polymerases switch during translesion DNA synthesis? *Mol Cell* **18**: 499-505.

608   Friedberg, E.C., Walker, G.C., Siede, W., Wood, R.D., Schultz, R.A., and Ellenberger, T. (2006)

609   Biological Responses to DNA Damage. In *DNA Repair and Mutagenesis*. Press, A. (ed).

610   Washington, D.C., pp. 3-7.

611   Grogan, D.W. (1998) Hyperthermophiles and the problem of DNA instability. *Molecular*

612   *Microbiology* **28**: 1043-1049.

613   Grogan, D.W. (2000) The question of DNA repair in hyperthermophilic archaea. *Trends*

614   *Microbiol* **8**: 180-185.

615   Grogan, D.W., Carver, G.T., and Drake, J.W. (2001) Genetic fidelity under harsh conditions:

616   analysis of spontaneous mutation in the thermoacidophilic archaeon Sulfolobus

617   acidocaldarius. *Proc Natl Acad Sci U S A* **98**: 7928-7933.

618   Grogan, D.W. (2004) Stability and repair of DNA in hyperthermophilic Archaea. *Curr Issues*

619   *Mol Biol* **6**: 137-144.

620   Gruz, P., Shimizu, M., Pisani, F.M., De Felice, M., Kanke, Y., and Nohmi, T. (2003) Processing

621   of DNA lesions by archaeal DNA polymerases from Sulfolobus solfataricus. *Nucleic*

622   *Acids Res* **31**: 4024-4030.

623   Gueguen, Y., Rolland, J.L., Lecompte, O., Azam, P., Le Romancer, G., Flament, D., Raffin, J.P.,

624   and Dietrich, J. (2001) Characterization of two DNA polymerases from the

625   hyperthermophilic euryarchaeon Pyrococcus abyssi. *Eur J Biochem* **268**: 5961-5969.

626   Haracska, L., Unk, I., Johnson, R.E., Johansson, E., Burgers, P.M., Prakash, S., and Prakash, L.

627   (2001) Roles of yeast DNA polymerases delta and zeta and of Rev1 in the bypass of

628   abasic sites. *Genes Dev* **15**: 945-954.

629   Henneke, G., Flament, D., Hubscher, U., Querellou, J., and Raffin, J.P. (2005) The

630   hyperthermophilic euryarchaeota Pyrococcus abyssi likely requires the two DNA

631   polymerases D and B for DNA replication. *J Mol Biol* **350**: 53-64.

632   Hoeijmakers, J.H. (2001) Genome maintenance mechanisms for preventing cancer. *Nature* **411**:

633   366-374.

634   Hogg, M., Wallace, S.S., and Doublie, S. (2004) Crystallographic snapshots of a replicative

635   DNA polymerase encountering an abasic site. *Embo J* **23**: 1483-1493.

636   Hubscher, U., Maga, G., and Spadari, S. (2002) Eukaryotic DNA polymerases. *Annu Rev*

637   *Biochem* **71**: 133-163.

638   Jacobs, K.L., and Grogan, D.W. (1997) Rates of spontaneous mutation in an archaeon from

639   geothermal environments. *J Bacteriol* **179**: 3298-3303.

640   Jin, Y.H., Ayyagari, R., Resnick, M.A., Gordenin, D.A., and Burgers, P.M. (2003) Okazaki

641   fragment maturation in yeast. II. Cooperation between the polymerase and 3'-5'-

642   exonuclease activities of Pol delta in the creation of a ligatable nick. *J Biol Chem* **278**:

643   1626-1633.

644   Jin, Y.H., Garg, P., Stith, C.M., Al-Refai, H., Sterling, J.F., Murray, L.J., Kunkel, T.A., Resnick,

645   M.A., Burgers, P.M., and Gordenin, D.A. (2005) The multiple biological roles of the 3'--

646   >5' exonuclease of Saccharomyces cerevisiae DNA polymerase delta require switching

647   between the polymerase and exonuclease domains. *Mol Cell Biol* **25**: 461-471.

648   Jolivet, E., Matsunaga, F., Ishino, Y., Forterre, P., Prieur, D., and Myllykallio, H. (2003)

649   Physiological responses of the hyperthermophilic archaeon "Pyrococcus abyssi" to DNA

650   damage caused by ionizing radiation. *J Bacteriol* **185**: 3958-3961.

651   Khare, V., and Eckert, K.A. (2002) The proofreading 3'-->5' exonuclease activity of DNA

652   polymerases: a kinetic barrier to translesion DNA synthesis. *Mutat Res* **510**: 45-54.

653   Kool, E.T. (2002) Active site tightness and substrate fit in DNA replication. *Annu Rev Biochem*

654   **71**: 191-219.

655   Kow, Y.W., and Dare, A. (2000) Detection of abasic sites and oxidative DNA base damage

656   using an ELISA-like assay. *Methods* **22**: 164-169.

657   Kroeger, K.M., Kim, J., Goodman, M.F., and Greenberg, M.M. (2006) Replication of an

658   oxidized abasic site in Escherichia coli by a dNTP-stabilized misalignment mechanism

659   that reads upstream and downstream nucleotides. *Biochemistry* **45**: 5048-5056.

660   Kubo, K., Ide, H., Wallace, S.S., and Kow, Y.W. (1992) A novel, sensitive, and specific assay

661   for abasic sites, the most commonly produced DNA lesion. *Biochemistry* **31**: 3703-3708.

662   Kuroita, T., Matsumura, H., Yokota, N., Kitabayashi, M., Hashimoto, H., Inoue, T., Imanaka, T.,

663   and Kai, Y. (2005) Structural mechanism for coordination of proofreading and

664   polymerase activities in archaeal DNA polymerases. *J Mol Biol* **351**: 291-298.

665   Lawrence, C.W., Borden, A., Banerjee, S.K., and LeClerc, J.E. (1990) Mutation frequency and

666   spectrum resulting from a single abasic site in a single-stranded vector. *Nucleic Acids Res*

667   **18**: 2153-2157.

668   Le Breton, M., Henneke, G., Norais, C., Flament, D., Myllykallio, H., Querellou, J., and Raffin,

669   J.P. (2007) The heterodimeric primase from the euryarchaeon Pyrococcus abyssi: a

670   multifunctional enzyme for initiation and repair? *J Mol Biol* **374**: 1172-1185.

671   Lindahl, T., and Nyberg, B. (1972) Rate of depuration of native deoxyribonucleic acid.

672   *Biochemistry* **11**: 3610-3618.

673   Lindahl, T. (1993) Instability and decay of the primary structure of DNA. *Nature* **362**: 709-715.

674   Loeb, L.A., Preston, B.D., Snow, E.T., and Schaaper, R.M. (1986) Apurinic sites as common

675   intermediates in mutagenesis. *Basic Life Sci* **38**: 341-347.

676   McCulloch, S.D., and Kunkel, T.A. (2006) Multiple solutions to inefficient lesion bypass by T7

677   DNA polymerase. *DNA Repair (Amst)* **5**: 1373-1383.

678   McGlynn, P., and Lloyd, R.G. (2002) Recombinational repair and restart of damaged replication

679   forks. *Nat Rev Mol Cell Biol* **3**: 859-870.

680   Myllykallio, H., Lopez, P., Lopez Garcia, P., Heilig, R., Saurin, W., Zivanovic, Y., Philippe, H.,

681   and Forterre, P. (2000) Bacterial mode of replication with eukaryotic-like machinery in a

682   hyperthermophilic archaeon. *Science* **288**: 2212-2215.

683   Nohmi, T. (2006) Environmental Stress and Lesion-Bypass DNA Polymerases. *Annu Rev*

684   *Microbiol*.

685   Pages, V., and Fuchs, R.P. (2002) How DNA lesions are turned into mutations within cells?

686   *Oncogene* **21**: 8957-8966.

687   Pages, V., Janel-Bintz, R., and Fuchs, R.P. (2005) Pol III proofreading activity prevents lesion

688   bypass as evidenced by its molecular signature within E.coli cells. *J Mol Biol* **352**: 501-

689   509.

690   Park, D. (2007) Genomic DNA isolation from different biological materials. *Methods Mol Biol*

691   **353**: 3-13.

692   Rothwell, P.J., and Waksman, G. (2005) Structure and mechanism of DNA polymerases. *Adv*

693   *Protein Chem* **71**: 401-440.

694 Rouillon, C., Henneke, G., Flament, D., Querellou, J., and Raffin, J.P. (2007) DNA Polymerase
695   Switching on Homotrimeric PCNA at the Replication Fork of the Euryarchaea
696   *Pyrococcus abyssi. J Mol Biol* **369**: 343-355.

697 Schaaper, R.M., and Loeb, L.A. (1981) Depurination causes mutations in SOS-induced cells.
698   *Proc Natl Acad Sci U S A* **78**: 1773-1777.

699 Schaaper, R.M., Kunkel, T.A., and Loeb, L.A. (1983) Infidelity of DNA synthesis associated
700   with bypass of apurinic sites. *Proc Natl Acad Sci U S A* **80**: 487-491.

701 Scharer, O.D., and Jiricny, J. (2001) Recent progress in the biology, chemistry and structural
702   biology of DNA glycosylases. *Bioessays* **23**: 270-281.

703 Shibutani, S., Takeshita, M., and Grollman, A.P. (1997) Translesional synthesis on DNA
704   templates containing a single abasic site. A mechanistic study of the "A rule". *J Biol*
705   *Chem* **272**: 13916-13922.

706 Shimizu, K., Hashimoto, K., Kirchner, J.M., Nakai, W., Nishikawa, H., Resnick, M.A., and
707   Sugino, A. (2002) Fidelity of DNA polymerase epsilon holoenzyme from budding yeast
708   Saccharomyces cerevisiae. *J Biol Chem* **277**: 37422-37429.

709 Shimizu, M., Gruz, P., Kamiya, H., Kim, S.R., Pisani, F.M., Masutani, C., Kanke, Y.,
710   Harashima, H., Hanaoka, F., and Nohmi, T. (2003) Erroneous incorporation of oxidized
711   DNA precursors by Y-family DNA polymerases. *EMBO Rep* **4**: 269-273.

712 Strauss, B.S. (1991) The 'A rule' of mutagen specificity: a consequence of DNA polymerase
713   bypass of non-instructional lesions? *Bioessays* **13**: 79-84.

714 Tanguy Le Gac, N., Delagoutte, E., Germain, M., and Villani, G. (2004) Inactivation of the 3'-5'
715   exonuclease of the replicative T4 DNA polymerase allows translesion DNA synthesis at
716   an abasic site. *J Mol Biol* **336**: 1023-1034.

717   Taylor, J.S. (2002) New structural and mechanistic insight into the A-rule and the instructional

718   and non-instructional behavior of DNA photoproducts and other lesions. *Mutat Res* **510**:

719   55-70.

720   Villani, G., Boiteux, S., and Radman, M. (1978) Mechanism of ultraviolet-induced mutagenesis:

721   extent and fidelity of in vitro DNA synthesis on irradiated templates. *Proc Natl Acad Sci*

722   *U S A* **75**: 3037-3041.

723   Yang, W. (2005) Portraits of a Y-family DNA polymerase. *FEBS Lett* **579**: 868-872.

724   Yang, W., and Woodgate, R. (2007) What a difference a decade makes: insights into translesion

725   DNA synthesis. *Proc Natl Acad Sci U S A* **104**: 15591-15598.

726   Zahn, K.E., Belrhali, H., Wallace, S.S., and Doublie, S. (2007) Caught bending the A-rule:

727   crystal structures of translesion DNA synthesis with a non-natural nucleotide.

728   *Biochemistry* **46**: 10551-10561.

729   Zhao, B., Xie, Z., Shen, H., and Wang, Z. (2004) Role of DNA polymerase eta in the bypass of

730   abasic sites in yeast cells. *Nucleic Acids Res* **32**: 3984-3994.

731   Zhao, H., Shen, J., Deininger, P., and Hunt, J.D. (2006) Abasic sites and survival in resected

732   patients with non-small cell lung cancer. *Cancer Lett*.

733

734

735 **FIGURE LEGENDS**

736 **Table 1. Damaged or intact oligonucleotides used in this study.** X represents the position of

737 the correct base, template C, or a tetrahydrofuran moiety designed to functionally mimic an

738 abasic site.

739

740 **Table 2**. **Incorporation kinetics by wild-type and exonuclease-deficient *Pab*pols.** Single

741 nucleotide insertion assays were performed as described in Experimental procedures. The

742 observed rates of deoxynucleotide incorporation as a function of dNTP concentration were firstly

743 determined from Lineweaver-Burk plots. The data were fit by nonlinear regression using the

744 Marquardt-Levenberg algorithm (EnzFitter 2.0, BioSoft) to the Michaelis-Menten equation

745 describing a hyperbola, $v = (V\text{max} \times [\text{dNTP}]/K\text{m} + [\text{dNTP}])$ as already described (Le Breton *et*

746 *al.*, 2007). Apparent Km and Vmax kinetic parameters were obtained from the fit and were used

747 to calculate the efficiency of deoxynucleotide incorporation (k_{cat}/K_m). The kinetics values are the

748 average of at least triplicate determinations and are shown with SD. The f(misinsertion

749 frequency) is the ratio k_{cat}/K_m for the incorrect nucleotide to k_{cat}/K_m for the correct nucleotide. ND

750 means no detectable incorporation observed.

751

752 **Figure 1. Rate of endogenous AP sites into *P. abyssi* and *E.coli* genomes at different growth**

753 **stages.** Steady-state level of AP sites per 100,000 bp was calculated during the exponential and

754 stationary phases of growth. The number of AP sites per 100,000 bp represents the mean of

755 triplicate experiments and error bars show the standard deviations of each measurement.

756

757 **Figure 2. Replication of AP sites containing M13mp18 DNA template by *Pab*pols. A,**

758 Chemical treatment to induced AP sites into M13mp18 DNA. **B,** Primer extension assays were

759 performed with 5'-fluorescein end labelled primer (oligonucleotide 6) hybridised to either the

760 damaged or undamaged M13mp18 DNA template, *Pab*pols and T4 DNA polymerase used as a

761 control experiment. The elongated products were separated on a 0.8 % (w/v) denaturing alkaline

762 agarose gel. Lanes 1, 2, 4, 6, 7, 9, 11, 12 are the undamaged extended products; lanes 3, 5, 8, 10,

763 13 are the damaged extended products. **C**, dNTPs incorporation into the damaged and

764 undamaged M13mp18 DNA primed-templates were tested by acid precipitation and incubation

765 was performed according to the dependent polymerase reactions with [^{3}H]dTTP as the substrate

766 (as outlined in Experimental procedures).

767

768 **Figure 3. Replication of AP-containing mini-circular and linear oligonucleotides DNA**

769 **templates by the wild-type or exonuclease-deficient *Pab*polB.** Primer extension assays were

770 performed at the indicated *Pab*polB concentrations with 8.3 nM of primer-template

771 (oligonucleotides 1 and 5), 200 µM dNTPs at 55°C for 30 min as described in the Experimental

772 procedures. Quantifications of the extended products from the AP site are mentioned below the

773 gels. The extent of the bypass reaction was calculated as the ratio of the intensity of the bands

774 downstream of the AP site to the intensity of the bands opposite the lesion. **A,** Replication onto

775 the AP site-containing linear template. The position of the abasic site is indicated by X. Lanes 2

776 and 9 correspond to the positive control with 8.3 nM of intact template (X=C). **B,** Replication of

777 the AP site-containing circular template. Lanes 2 and 8 correspond to the positive control with

778 8.3 nM of intact template (X=C). 32 mer indicates the position of the base preceding the AP site,

779 while 33 mer is the position of the AP site.

780

781 **Figure 4. Replication of AP-containing mini-circular and linear oligonucleotides DNA**

782 **templates by the wild-type or exonuclease-deficient *Pab*polD.** Primer extension assays were

783 performed at the indicated *Pab*polD concentrations with 8.3 nM of primer-template

784 (oligonucleotides 1 and 5), 200 µM dNTPs at 55°C for 30 min as described in the Experimental

785 procedures. Quantification of the extended products from the AP site is mentioned below the

786 gels. The extent of the bypass reaction was calculated as the ratio of the intensity of the bands

787 downstream of the AP site to the intensity of the bands opposite the lesion. **A,** Replication onto

788 the AP site-containing linear template. The position of the abasic site is indicated by X. Lanes 2

789 and 8 correspond to the positive control with 8.3 nM of template (X=C). **B,** Replication of the

790 AP site-containing circular template. Lanes 2 and 8 correspond to the positive control with 8.3

791   nM of template (X=C). 32 mer indicates the position of the base preceding the AP site, while 33

792   mer is the position of the AP site.

793

794   **Figure 5. Effect of varying the downstream template base on nucleotide incorporation**

795   **opposite an AP site by *Pab*pols.** Standing start reactions were performed with four DNA

796   templates that varied by the nature of the 5' template base. The fluorescein-labelled primer

797   (oligonucleotide 6) was annealed right before the template AP site that is indicated by X.

798   Different template bases 5′ to the AP site are depicted by N (N=A, oligonucleotide 2; N=T,

799   oligonucleotide 1; N=G, oligonucleotide 3; N=C, oligonucleotide 4) (Table 1). Single nucleotide

800   incorporations were carried out as described in Experimental procedures with the different

801   primed-templates, 13 nM of *Pab*polB exo+/exo-, 20 nM of *Pab*polD exo+/exo-, 200 µM of each

802   dNTP at 55°C for 30 min. A. Reaction with 13 nM *Pab*polB exo+. B. Reaction with 20 nM

803   *Pab*polD exo+. C. Reaction with 13 nM *Pab*polB exo-. D. Reaction with 20 nM *Pab*polD exo+.

804

Oligonucleotide 1

5'-CAGGAAACAGCTATGACCATGATTACGAATTCGAGCTCGGTACCCGGGGATCC**TX**TAGAGTCGACCTGCAGGCATGCAAGCTTGGCA-3'

Oligonucleotide 2

5'-CAGGAAACAGCTATGACCATGATTACGAATTCGAGCTCGGTACCCGGGGATCC**AX**TAGAGTCGACCTGCAGGCATGCAAGCTTGGCA-3'

Oligonucleotide 3

5'-CAGGAAACAGCTATGACCATGATTACGAATTCGAGCTCGGTACCCGGGGATCC**GX**TAGAGTCGACCTGCAGGCATGCAAGCTTGGCA-3'

Oligonucleotide 4

5'-CAGGAAACAGCTATGACCATGATTACGAATTCGAGCTCGGTACCCGGGGATCC**CX**TAGAGTCGACCTGCAGGCATGCAAGCTTGGCA-3'

Oligonucleotide 5

5'-TGCCAAGCTTGCATGCC-3'

Oligonucleotide 6

5'-TGCCAAGCTTGCATGCCTGCAGGTCGACTCTA-3'

805
806   **Table 1 : Damaged or intact oligonucleotides used in this study**

807

	DNA polymerase	dNTP	Km (μM)	$kcat$ (min^{-1})	$kcat/Km$ (μM^{-1} min^{-1})	f(misinsertion frequency)
Insertion opposite C	*Pab*polB exo+	dATP	ND	ND	ND	
		dTTP	ND	ND	ND	
		dGTP	0.25±0.01	425.27 ±0.12	1671.5	
		dCTP	ND	ND	ND	
	*Pab*polD exo+	dATP	ND	ND	ND	
		dTTP	ND	ND	ND	
		dGTP	0.19±0.02	66.70±0.69	346.36	
		dCTP	ND	ND	ND	
	*Pab*polB exo-	dATP	18.70±1.23	61.09±0.43	3.27	0.11
		dTTP	5.46±0.05	35.05±0.86	6.42	0.21
		dGTP	1.98±0.35	60.29±0.15	30.41	1.00
		dCTP	32.01±2.11	23.07±0.37	0.72	0.02
	*Pab*polD exo-	dATP	74.47±9.16	39.71±1.28	0.53	0.16
		dTTP	17.00±3.50	32.50±1.30	1.91	0.57
		dGTP	13.93±1.08	46.81±8.60	3.36	1.00
		dCTP	374.69±129.32	10.41±8.20	0.03	0.01
Insertion opposite AP site	*Pab*polB exo+	dATP	100±9	87±4	0.79	
		dTTP	121±7	91±4	0.75	
		dGTP	610±40	120±8	0.20	
		dCTP	ND	ND	ND	
	*Pab*polD exo+	dATP	36±3	114±4	3.17	
		dTTP	650±20	102±2	0.16	
		dGTP	ND	ND	ND	
		dCTP	ND	ND	ND	
	*Pab*polB exo-	dATP	4.19±0. 31	89.42±1.23	21.35	
		dTTP	15.02±0. 18	62.92±0. 11	4.19	
		dGTP	8.88± 2.35	73.68±4.71	8.30	
		dCTP	ND	ND	ND	
	*Pab*polD exo-	dATP	12.00±2.41	29.03±1.32	2.42	
		dTTP	76.19±0. 85	25.55±0. 07	0.34	
		dGTP	70.41±7.61	12.43±0. 36	0.18	
		dCTP	82.08±6.12	30.72±0. 54	0.37	

808
809
810 **Table 2 : Incorporation kinetics by wild-type and exonuclease-deficient *Pab*pols**

811
812

Figure1

Figure 2

A.

M13mp18 DNA without lesions $\xrightarrow{\text{45 min-70 °C}}$ Apurinic M13mp18 DNA

Sodium citrate (10 mM)

Potassium chloride (30 mM, pH 3)

B.
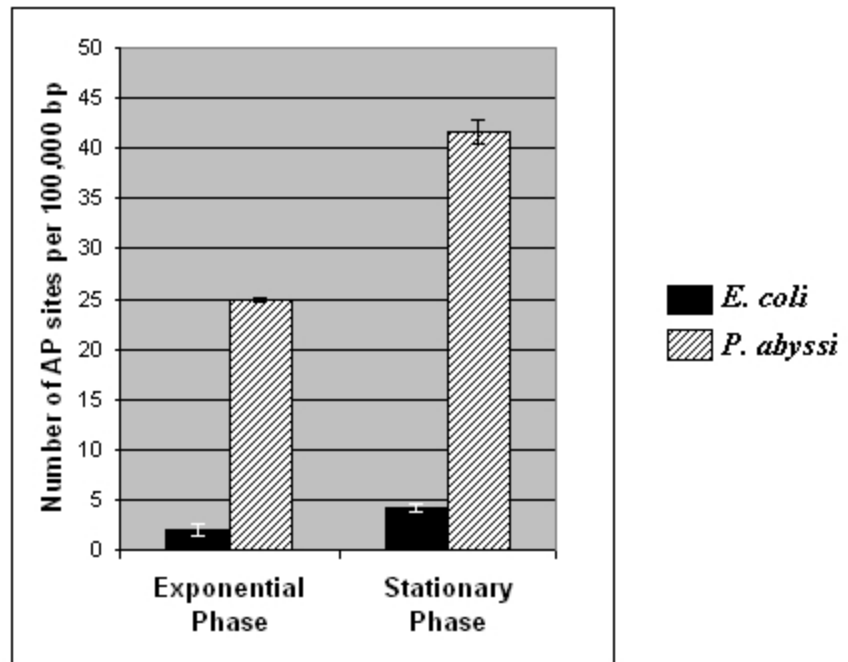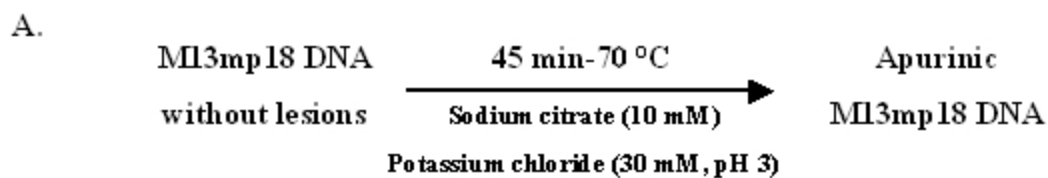
	1	2	3	4	5	6	7	8	9	10	11	12	13
M13mp18	+	+	-	+	-	+	+	-	+	-	+	+	-
AP-M13mp18	-	-	+	-	+	-	-	+	-	+	-	-	+
T4DNA pol	-	-	-	-	-	-	-	-	-	-	-	+	+
*Pab*polD exo+	-	-	-	-	-	-	+	+	-	-	-	-	-
*Pab*polD exo-	-	-	-	-	-	-	-	-	+	+	-	-	-
*Pab*polB exo+	-	+	+	-	-	-	-	-	-	-	-	-	-
*Pab*polB exo-	-	-	-	+	+	-	-	-	-	-	-	-	-

(M13mp18) 7,249-nt ——

3,600-nt ——

2,319-nt ——

700-nt ——

C.

Bar chart legend: □ AP-M13mp18 ▪ M13mp18

Y-axis categories (top to bottom): T4DNA pol, *Pab*polB exo+, *Pab*polB exo-, *Pab*polD exo+, *Pab*polD exo-

X-axis: 0 20 40 60 80 100 120 140 160 180 200 (pmol/30 min)
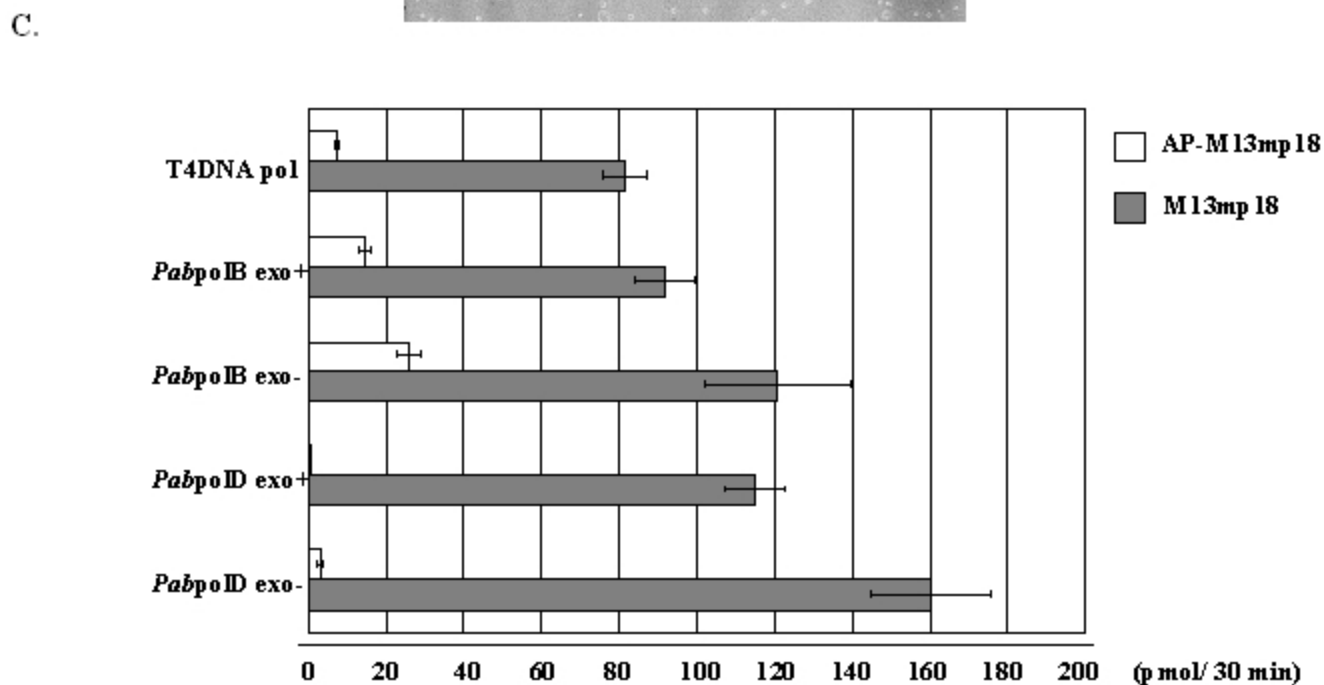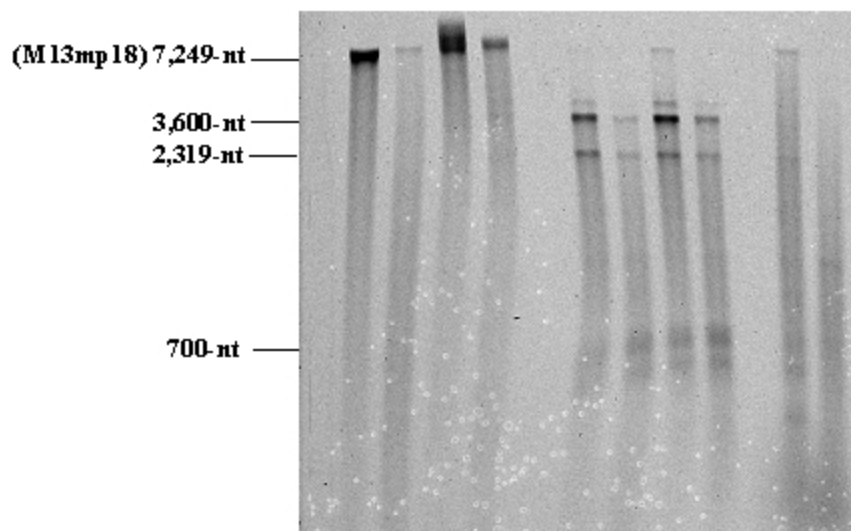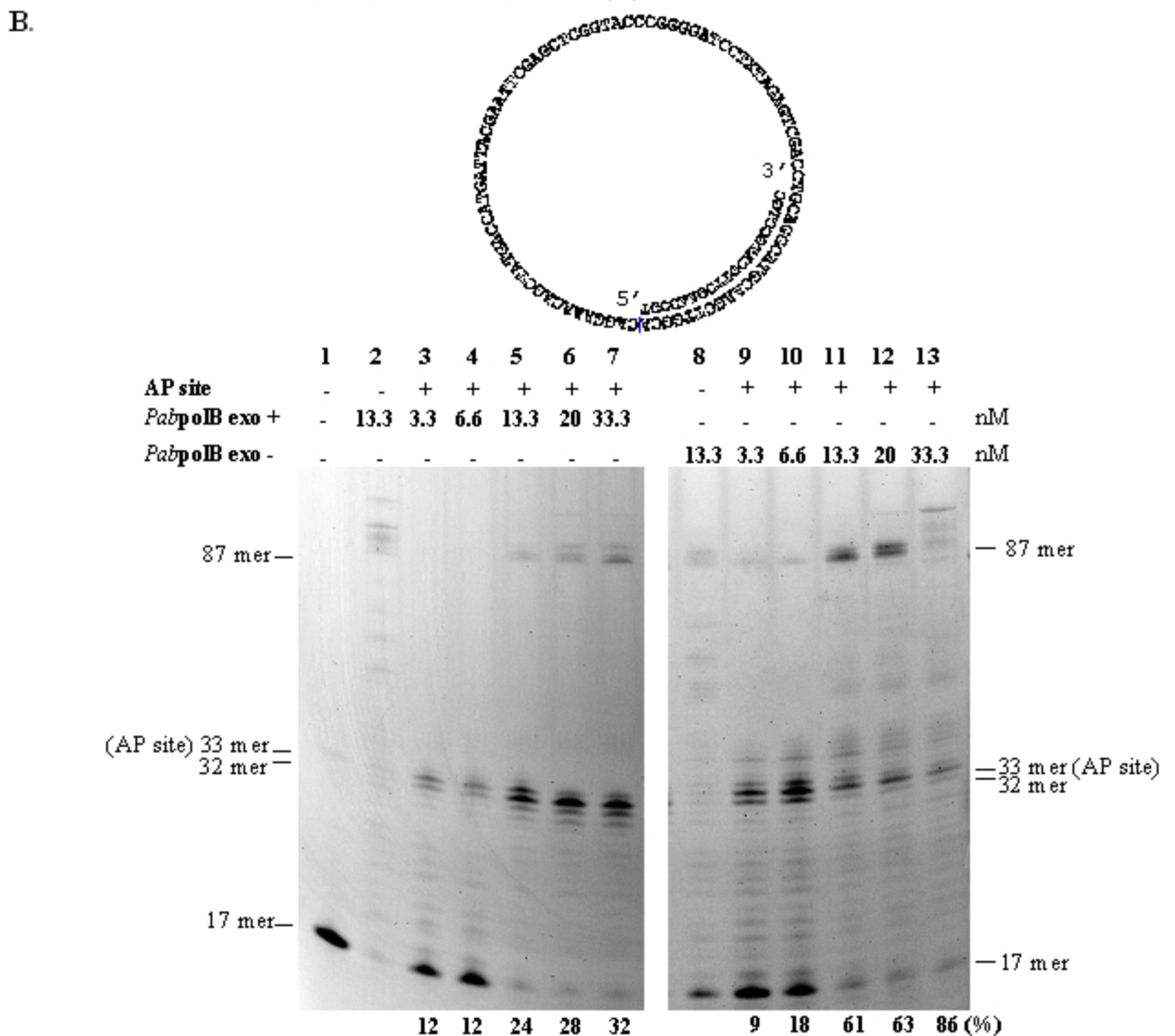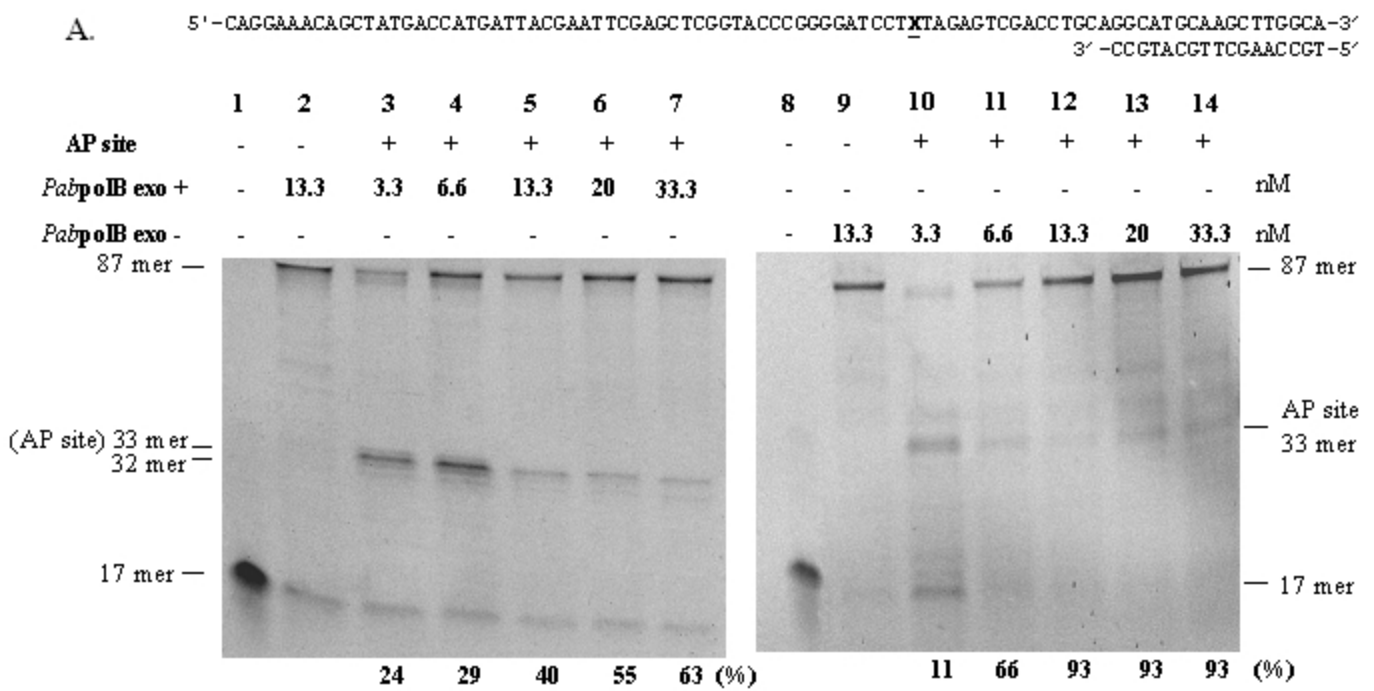
Figure 3

A.

5'-CAGGAAACAGCTATGACCATGATTACGAATTCGAGCTCGGTACCCGGGGATCCT**X**TAGAGTCGACCTGCAGGCATGCAAGCTTGGCA-3'

3'-CCGTACGTTCGAACCGT-5'

	1	2	3	4	5	6	7	8	9	10	11	12	13	
AP site	-	-	+	+	+	+	+	-	+	+	+	+	+	
*Pab*polD exo +	-	20	3.3	6.6	13.3	20	33.3	-	-	-	-	-	-	nM
*Pab*polD exo -	-	-	-	-	-	-	-	20	3.3	6.6	13.3	20	33.3	nM

                                    31 31 35 (%)

B.

	1	2	3	4	5	6	7	8	9	10	11	12	13	
AP site	-	-	+	+	+	+	+	-	+	+	+	+	+	
*Pab*polD exo +	-	20	3.3	6.6	13.3	20	33.3	-	-	-	-	-	-	nM
*Pab*polD exo -	-	-	-	-	-	-	-	20	3.3	6.6	13.3	20	33.3	nM

                              16 48 73 73 80 (%)

Figure 4 : Replication of AP-containing mini-circular and linear oligonucleotides DNA templates by the wild-type or exonuclease-deficient *Pab*polD

5'-CAGGAAACAGCTATGACCATGATTACGAATTCGAGCTCGGTACCCGGGGATCC**NX**TAGAGTCGACCTGCAGGCATGCAAGCTTGGCA-3'
ATCTCAGCTGGACGTCCGTACGTTCGAACCGT-5'

dNTP

A.

Pab pol B exo+

B.

Pab pol D exo+

C.

Pab pol B exo-

D.

Pab pol D exo-

Figure 5

Figure S1: Mapping of conserved residues involved in 3'-5' exonuclease activity among representative euryarchaeal DNA polymerases.
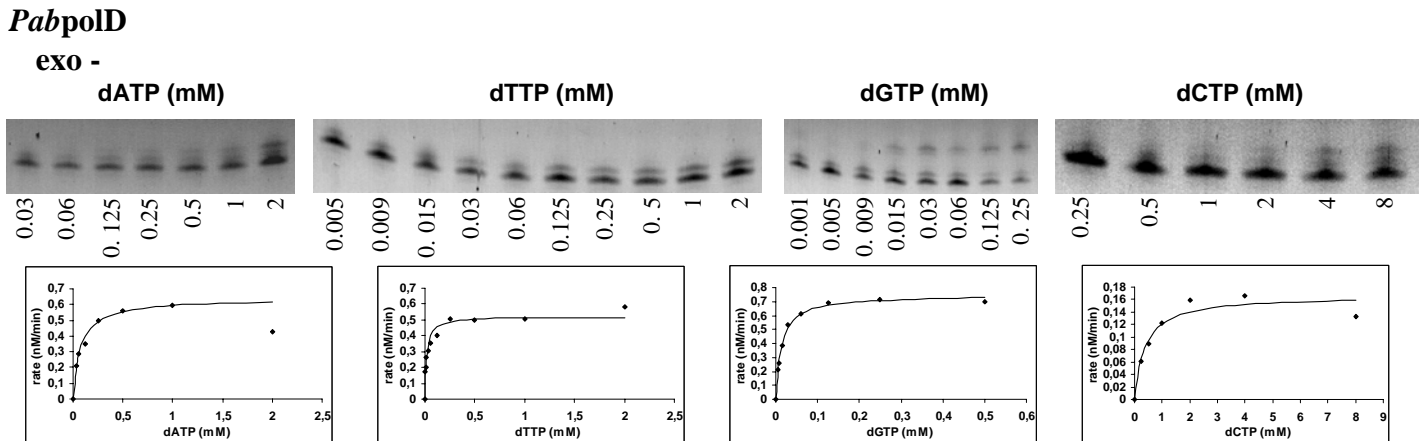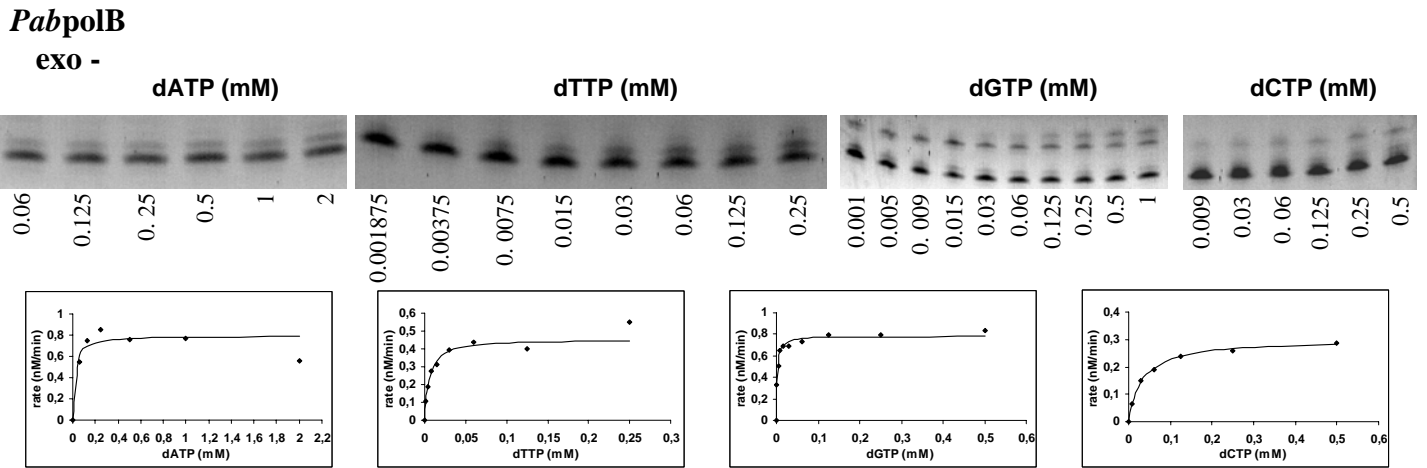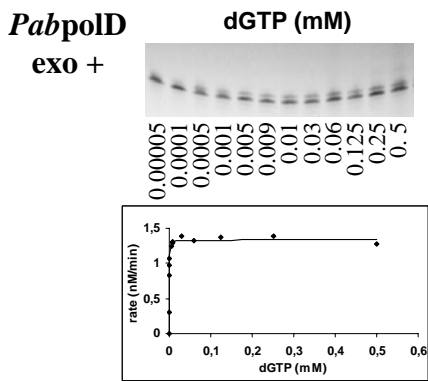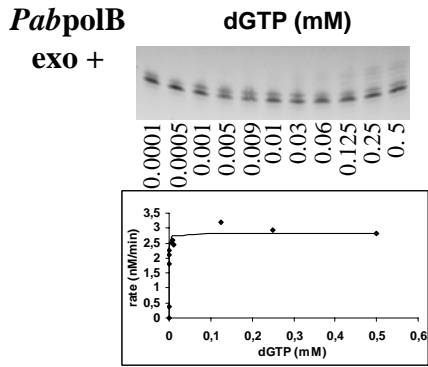**A**, Sequence alignment of the exonuclease domain in representative family B DNA polymerases. The sequences are from eight euryarchaeota species, *P. abyssi* (Pab, accession number, gi:14521919), *P. furiosus* (Pfu, accession number, gi:18976584), *P. horikoshii* (Pho, accession number, gi:14591688), *T. kodakarensis* KOD1 (Tko, accession number, gi:57639936), *M. thermoautotrophicum* (Mth, accession number, gi:15679219), *M. jannashii* (Mja, accession number, gi:15669075), *A. fulgidus* (Afu, accession number, gi:11498108), *T. acidophilum* (Tac, accession number, gi:16081956). The star indicates the identified residue in *Pab*polB responsible for proofreading activity. **B**, Partial sequence alignment of the small subunits (DP1s) of the family D DNA polymerases. The sequences are from eight euryarchaeota species, *P. abyssi* (Pab, accession number, gi:14520339), *P. furiosus* (Pfu, accession number, gi:18976390), *P. horikoshii* (Pho, accession number, gi:14590067), *T. kodakarensis* KOD1 (Tko, accession number, gi:57641837), *M. thermoautotrophicum* (Mth, accession number, gi:15679404), *M. jannashii* (Mja, accession number, gi:15668883), *A. fulgidus* (Afu, accession number, gi:11499379), *T. acidophilum* (Tac, accession number, gi:16081371). The star indicates the identified residue in *Pab*DP1 responsible for proofreading activity. Amino acid sequence alignments have been constructed by ClustalW2. Numbering refers to *P. abyssi* amino acid sequences.
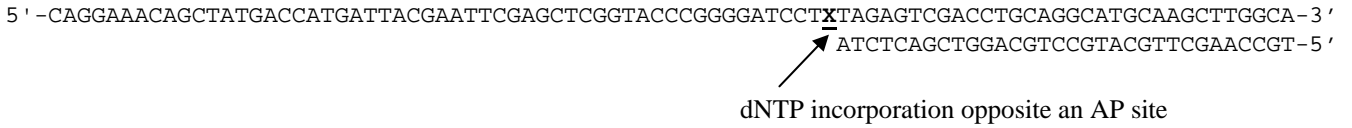
A.

5'-CAGGAAACAGCTATGACCATGATTACGAATTCGAGCTCGGTACCCGGGGATCCT**C**TAGAGTCGACCTGCAGGCATGCAAGCTTGGCA-3'
ATCTCAGCTGGACGTCCGTACGTTCGAACCGT-5'

dNTP incorporation opposite undamaged nucleotide C

B.

5'-CAGGAAACAGCTATGACCATGATTACGAATTCGAGCTCGGTACCCGGGGATCCT**X**TAGAGTCGACCTGCAGGCATGCAAGCTTGGCA-3'
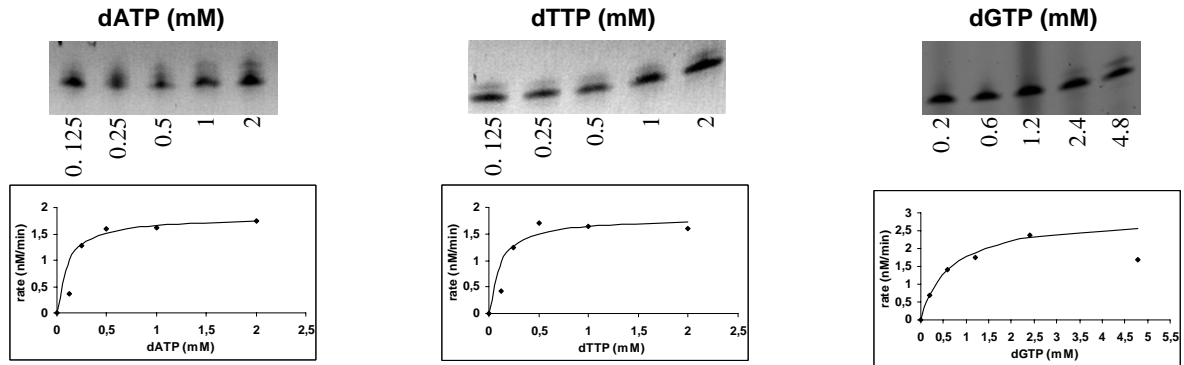ATCTCAGCTGGACGTCCGTACGTTCGAACCGT-5'

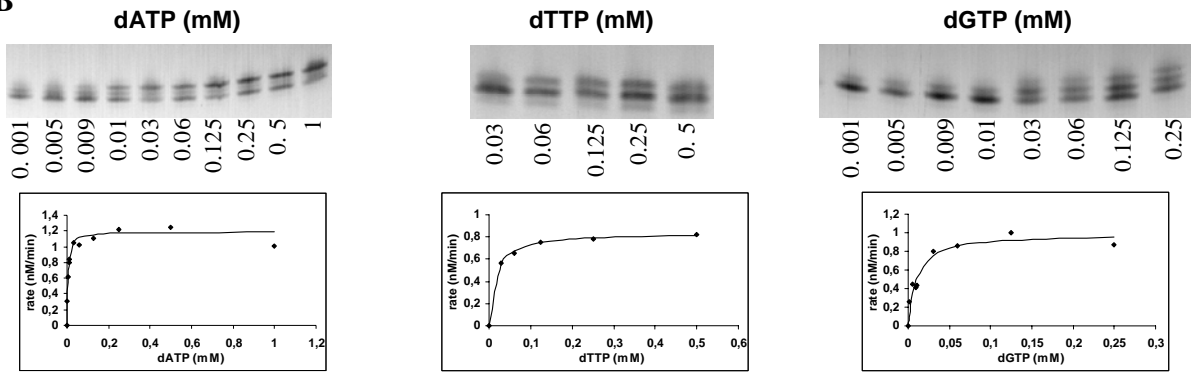dNTP incorporation opposite an AP site

*Pab*polB
exo +
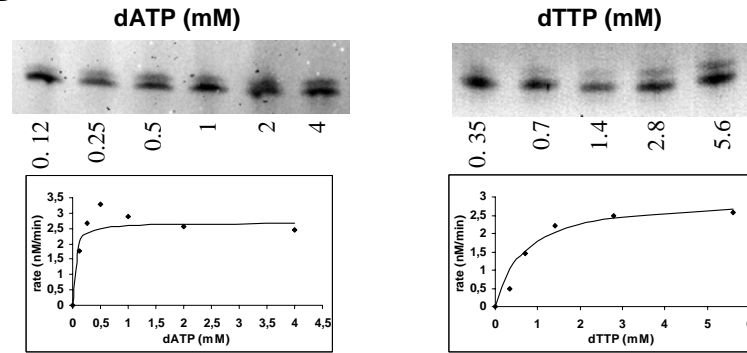
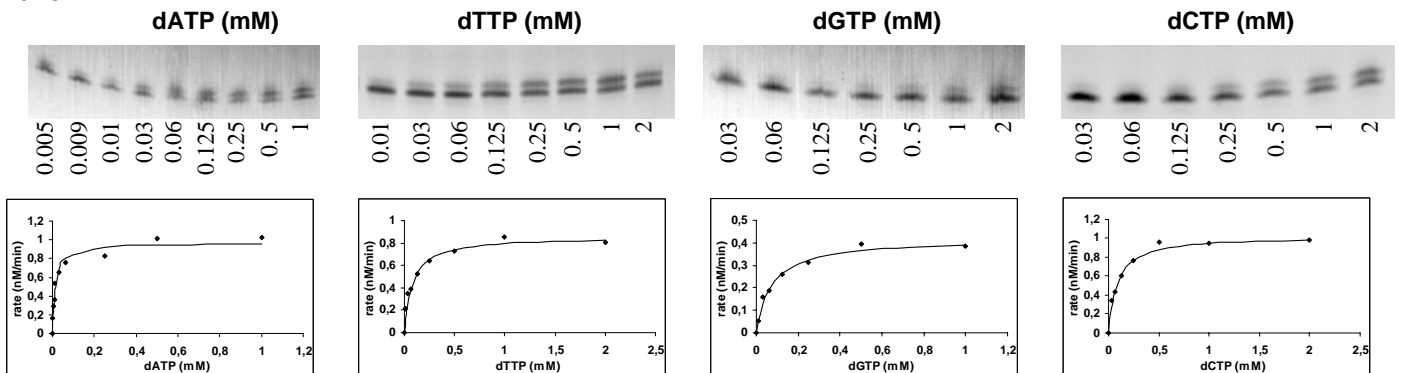
*Pab*polD
exo +

*Pab*polB
exo -

*Pab*polD
exo -

Figure S2: Steady-state kinetics analyses of deoxynucleotide incorporation by *Pab*pols.
A, Incorporation of dNTP opposite undamaged C. The primer-template duplex (8.3 nM) was incubated individually with *Pab*polB exo+ (6.6 nM), *Pab*polD exo+ (20 nM), *Pab*polB exo- (13 nM) or *Pab*polD exo- (16 nM), in the presence of a single dNTP at the indicated concentrations. **B**, Incorporation of dNTP opposite an AP site. The primer-template duplex (8.3 nM) was incubated individually with *Pab*polB exo+ (24 nM), *Pab*polD exo+ (20 nM), *Pab*polB exo- (13.3 nM) or *Pab*polD exo- (33.3 nM), in the presence of a single dNTP at the indicated concentrations. Reactions were carried out at 55°C under standard *Pab*pols assay conditions and the products were resolved by denaturing PAGE. The rate of incorporation was graphed as a function of dNTP concentration and the data were fit to the Michaelis-Menten equation. The k_{cat} et K_m parameters obtained from the fit are listed in Table 2.